

Responses to Referee #1's comments

The authors have addressed my two major concerns from the last review and have done a considerable amount of work showing robustness in their results. Overall I find the paper acceptable for publication and I commend the authors on all their hard work to untangle aerosol-precipitation effects in this interesting study.

The segregation of data into polluted/clean moist/dry days is very compelling and I appreciate their additional work on the arduous work of calculating CDNC.

Reply: Thanks.

Figure 6 is very compelling. The authors could consider using a 2d-bivariate kernel density estimate (<https://seaborn.pydata.org/generated/seaborn.kdeplot.html>) to visualize the density of the relatively sparse data points for additional punch to the figure, but this is totally optional and I find the figure convincing as is.

Reply: Thanks for suggesting this method. However, the 2d-PDF plot overlaps and not as clear as Figure 6, so we keep Figure 6 as it is.

One thing that would be interesting (but not essential) would be to examine if total rainfall over a day is affected by CDNC, or if it's just onset, etc. That is to say, does accumulated rainfall care at all about CDNC, or is it just driven by moisture? If this is not the case this would be worth noting for comparison to other studies.

Reply: Intuitively, both the CDNC and moisture affect the total rainfall throughout the day. Table below shows the total rainfall over a day categorized individually by CDNC and specific humidity at 850 hPa. It therefore implies that moisture has larger influence on the daily rainfall amount.

Total rainfall over a day (mm)	CDNC<25 th	CDNC>75 th	SH<25 th	SH>75 th
Average for heavy rainfall	29.3	33.9	25.6	35.6
Average for total rainfall	11.8	12.4	7.2	17.0

Table S1. Averaged total rainfall over a day (mm/day) classified by CDNC and SH.

Table 1-5. Might be good to give standard error on the means. Not essential.

Reply: We have added standard deviations in Table 2-5.

Responses to Referee #2's comments

The authors have done a significant amount of work improving the manuscript. The precipitation part of this paper is interesting and I think worthy of publication. However, some of my concerns remain, particularly in regards to the detection of causal relationships and the use of the CDNC.

Aerosol-cloud-precipitation relationships

I understand that it is difficult to control for meteorological covariations and systematic biases when performing these observational studies and I appreciate the extra section on the impact of humidity that the authors have included. Section 3.3 (and 4.2) is a useful addition to the paper, especially given that the paper is dealing with a difficult subject. However, it seems that the results from section 3.3 do not make it to the abstract and conclusions, which still give the impression that aerosols have been shown to cause these changes in cloud and precipitation properties. Where these results from section 3.3 are mentioned (e.g. in the abstract, L49-51), it is almost as an afterthought, failing to point out that the impact of moisture changes is the same as the impact of sulphate, which means that the aerosol effect cannot be isolated from the impact of humidity.

Reply: Yes, it is our oversight, and now the abstract and conclusions cover these points reminded by the Reviewer, see L45, 49-50, 559-562.

It has previously been shown that using reanalysis moisture variables cannot completely control for meteorological covariations between aerosol and precipitation (Boucher and Quaas, 2012). In addition, several of the relationships examined within section 4 are known to be affected by meteorological covariations: AOD-CF (Quaas et al., 2010; Grandey et al., 2013) and AOD-CTP (Gryspeerd et al., 2014). Where these relationships are discussed in this paper (e.g. L521 onwards), they appear to be used as evidence for an aerosol effect on cloud, despite these known issues.

Reply: We agree, and have re-written the text to reflect the points, see L540-546 in section 5.2.

This is not a large change to the paper, mostly just in the abstract and conclusions (e.g. changing sentences such as L547 - '... the different roles of [aerosol] in modifying the diurnal ...' to '... the different relationships of [aerosol] to the diurnal ...'). I also would suggest that the discussion in section 5, particularly around the relationships between AOD and cloud properties, is modified to reflect the previous results.

Reply: See above.

CDNC retrieval

My fourth point in the previous review mentioned that it is not clear that the CDNC-CER and CDNC-COT relationships are useful, as they are not independent. The response suggests that these have been removed, but investigation of the CDNC-CER relationship is still present and compared with the AOD-CER relationship (e.g. L360, L521, L532). There may be a justification for including the CDNC-CER relationship (I am not clear that it has to be removed), but could the authors clarify whether they are removing it or not?

Reply: We agree and have removed the CDNC-CER/COT versus AOD comparison in sections 4.1 and 5.2. Because we believe that the increased liquid COT and decreased liquid CER may be not completely caused by CDNC calculation but the effect of CCN (which is explained in section 4.2 L407-409), these results remain in the figure 7 and table 4 for reference.

It is good to include the reference to the Grosvenor paper and a discussion of the uncertainties. However, I am not sure the impact of the uncertainties on the results is addressed. In particular, the CDNC retrieval is for adiabatic clouds, and it is not clear that it can be applied to convective clouds. Clouds that are raining are by definition non-adiabatic. How does this affect the results in this work? Might it reduce the significance of the results?

Reply: The use of CDNC is to provide corroborative evidence for the results based on AOD. We understand the issue and uncertainties of “adiabatic” clouds, however, we believe that it does not affect the major findings of this study. Anyway, we added additional statement to highlight it, see L496-497.

Section 4 starts referring to the CDNC as CCN. Is this appropriate? CDNC depends on CCN and updraught, presumably there is a strong variation in updraught between convective clouds which weakens the link between CDNC and CCN?

Reply: In this study, we use CDNC as a surrogate for CCN, while the issue of updraught, although important, is outside the scope of this study. Nevertheless, for clarification, we have modified the statements in section 4.

The average values for the retrieved CDNC (L391) are very high (more than 2000 cm⁻³). For an optical depth of 100, this would mean that all of the effective radius retrievals are smaller than around 6µm. Is this correct?

Reply: This question prompted us to double check the results. As it turns out that we made an error in the CDNC unit conversion from the units of C_w , ρ_w , and R_e having gm^{-4} , kgm^{-3} , and μm respectively. So the value of CDNC (=2000) should be reduced by $10^{3/2}$ ($10^{15/2}$ versus 10^9) cm^{-3} to a value of 63.2 cm^{-3} , and we have revised the values in L390-391 and Table 1. This error nevertheless does not affect other results. In any case, we deeply appreciate this comment.

Following my third point in the previous review, it is not clear how the CDNC is calculated. Are the 1 by 1 degree mean values of CER and COT used? If so, this should be noted, as it may cause an underestimate in the CDNC compared to other studies (e.g. Quaas et al., 2008;

Grandey et al., 2010) which use the level 2 data or the L3 joint histogram 'Cloud_Optical_Thickness_Liquid_JHisto_vs_Eff_Radius' to calculate the CDNC.

Reply: We used 1 by 1 degree mean values of CER and COT of L3 cloud product of MODIS. We have clarified the data use in L182-184. However, we are not sure if the CDNC is underestimated since both COT and CER may be underestimated.

Minor points

L442 - Ackerman (2000) is a usual reference for the semi-direct effect.

Reply: Thanks for the reference, we have added it (L443).

L470 - 'absorbing aerosol effect' -> 'absorbing aerosol results'? I am not sure that an effect is specified (to me, it would require some kind of process being suggested)

Reply: We have modified the statements, see L300, 302-303, 470-471.

Section 4.2 - repeated references to section 5.1, when presumably 4.1 is meant?

Reply: I understand what you mean is in L398 and L433 that 5.1 should be 4.1, we have revised it.

L500 - Relative changes are still subject to systematic biases, which are the more important source of error in a study like this.

Reply: We have modified the sentence, see L502-504.

L510 - I understand that these datasets are the best available. However, if they are insufficient to demonstrate a causal effect of aerosol on cloud or precipitation properties, then they are insufficient. In that case, this must be noted.

Reply: We agree and added sentence about it, see L512-516.

L520 - Or sampling differences between the AOD and CDNC?

Reply: We agree and added it, see L524.

L539 - What happened to section 6?

Reply: Revised, see L548.

Fig. 8 - The units for the x-axis are "%" only

Reply: Revised, see Figure 8.

There are still some spelling/grammar issues (e.g. black carbons - L44 and in the new sections), but they don't appear to make too difficult to understand the paper and could be corrected in proof reading.

Reply: We have carefully checked the manuscript again and corrected some mistakes.

References

Ackerman, A. S. (2000), *Reduction of Tropical Cloudiness by Soot*, *Science*, 288(5468), 10421047, doi:10.1126/science.288.5468.1042.

Boucher, O., and J. Quaas (2012), *Water vapour affects both rain and aerosol optical depth*, *Nat. Geosci.*, 6(1), 45, doi:10.1038/ngeo1692.

Grandey, B. S., and P. Stier (2010), *A critical look at spatial scale choices in satellite-based aerosol indirect effect studies*, *Atmos. Chem. Phys.*, 10(23), 1145911470, doi:10.5194/acp-10-11459-2010.

Grandey, B. S., P. Stier, and T. M. Wagner (2013), *Investigating relationships between aerosol optical depth and cloud fraction using satellite, aerosol reanalysis and general circulation model data*, *Atmos. Chem. Phys.*, 13(6), 31773184, doi:10.5194/acp-13-3177-2013.

Gryspeerd, E., P. Stier, and B. S. Grandey (2014), *Cloud fraction mediates the aerosol optical depth-cloud top height relationship*, *Geophys. Res. Lett.*, 41, 36223627, doi:10.1002/2014GL059524.

Quaas, J., O. Boucher, N. Bellouin, and S. Kinne (2008), *Satellite-based estimate of the direct and indirect aerosol climate forcing*, *J. Geophys. Res.*, 113, 05204, doi:10.1029/2007JD008962.

Quaas, J., B. Stevens, P. Stier, and U. Lohmann (2010), *Interpreting the cloud cover aerosol optical depth relationship found in satellite data using a general circulation model*, *Atmos. Chem. Phys.*, 10(13), 61296135, doi:10.5194/acp-10-6129-2010.

Rosenfeld, D. et al. (2016), *Satellite retrieval of cloud condensation nuclei concentrations by using clouds as CCN chambers.*, *P. Natl. Acad. Sci. USA*, 113(21), 582834, doi:10.1073/pnas.1514044113.

1 **An observational study of the effects of aerosols on diurnal variation of heavy rainfall**
2 **and the concurrent cloud changes over Beijing-Tianjin-Hebei**

3
4 Siyuan Zhou^{1,2,3}, Jing Yang^{1,2*}, Wei-Chyung Wang³, Chuanfeng Zhao⁴, Daoyi Gong^{1,2}, Peijun Shi^{1,2}

5
6 ¹State Key Laboratory of Earth Surface Process and Resource Ecology, Beijing Normal University, China

7 ²Key Laboratory of Environmental Change and Natural Disaster, Faculty of Geographical Science, Beijing
8 Normal University, China

9 ³Atmospheric Sciences Research Center, State University of New York, Albany, New York 12203, USA

10 ⁴College of Global Change and Earth System Science, Beijing Normal University, China

11
12
13 Submitted to ACP
14 Oct 2018

15
16
17
18
19
20
21
22
23
24
25
26
27
28
29
30
31
32
33 *Correspondence to: Jing Yang, State Key Laboratory of Earth Surface Process and Resource Ecology/Key
34 Laboratory of Environmental Change and Natural Disaster, Faculty of Geographical Science, Beijing Normal
35 University, 19#Xinjiekouwai Street, Haidian District, Beijing 100875, China. E-mail: yangjing@bnu.edu.cn

思媛 周 19/7/21 12:02 AM

已删除: Yang^{2,3}

思媛 周 19/7/21 12:02 AM

已删除: Wang⁴

思媛 周 19/7/21 12:02 AM

已删除: Zhao^{3,5}

思媛 周 19/7/21 12:02 AM

已删除: Gong^{2,3}

思媛 周 19/7/21 12:02 AM

已设置格式: 上标

思媛 周 19/7/21 12:02 AM

已删除: Shi^{2,3}

思媛 周 19/7/21 12:02 AM

已删除: ¹ Key Laboratory of Environmental Change and Natural Disaster, Beijing Normal University, China
⁴Atmospheric

思媛 周 19/7/21 12:02 AM

已设置格式: 字体颜色: 自动

思媛 周 19/7/21 12:02 AM

已设置格式: 字体颜色: 自动, 突出显示

思媛 周 19/7/21 12:02 AM

已删除: ⁴Atmospheric

思媛 周 19/7/21 12:02 AM

已删除: ⁵

思媛 周 19/7/21 12:02 AM

已删除: Academy

思媛 周 19/7/21 12:02 AM

已设置格式: 字体颜色: 自动, 英语(英国)

思媛 周 19/7/21 12:02 AM

已设置格式: 字体颜色: 自动, 英语(英国)

思媛 周 19/7/21 12:02 AM

已删除: Reduction and Emergency Management

50 **Abstract:** Our previous study found that the observed rainfall diurnal variation over Beijing-Tianjin-Hebei
51 shows distinct signature of the effects of pollutants. Here we used the hourly rainfall data together with
52 satellite-based daily information of aerosols and clouds to further investigate the effects of aerosols on heavy
53 rainfall, and the concurrent changes of cloud properties. For heavy rainfall, three distinguished characteristics
54 are identified: *earlier start time*, *earlier peak time*, and *longer duration*. The quantitative values of these
55 changes are however sensitive to the choice of pollution indicators: 0.7, 1.0 and 0.8 hours based on aerosol
56 optical depth (AOD); and 2.1, 4.2 and 2.4 hours based on cloud droplet number concentration (CDNC).
57 In-depth analysis suggests that the characteristics of earlier in both start time and peak time occur in the
58 presence of black carbon (absorbing aerosols) while the longer duration is attributed to sulfate (scattering
59 aerosols) and increased low-level moisture (specific humidity at 850 hPa). Because of its close relevance to
60 changes in heavy rainfall, we also examined changes of clouds. Significant increases in cloud fraction, cloud
61 top pressure, the liquid/ice cloud optical thickness and cloud water path are exhibited. The liquid cloud
62 effective radius is increased using AOD while the ice cloud effective radius is decreased using either AOD or
63 CDNC. The moisture has the similar effect on cloud with the CDNC, which means that the aerosol effect may
64 not be isolated from the impact of humidity. Finally, the mechanisms which may explain the aerosol effects are
65 discussed and hypothesized.

66 **Key words:** aerosol, heavy rainfall, diurnal variation, cloud, Beijing-Tianjin-Hebei, observational study

67

68 1. Introduction

69 Aerosols modify the global hydrologic cycle through both radiative effect (direct effect) and cloud effect
70 (indirect effect) (IPCC, 2013). On the one hand, through absorbing or scattering solar radiation, aerosols can
71 lead to the air aloft heating (e.g. Jacobson 2001; Lau et al. 2006) or the surface cooling (Lelieveld and
72 Heintzenberg 1992; Guo et al. 2013; Yang et al., 2018), which changes the atmospheric vertical static stability
73 and modulates rainfall (e.g. Rosenfeld et al. 2008). On the other hand, water-soluble aerosols serving as cloud
74 condensation nuclei (CCN) could affect the warm-rain processes and cold-rain processes through influencing
75 the cloud droplet size distributions, cloud top heights and other cloud properties (Jiang et al., 2002; Givati and
76 Rosenfeld 2004; Chen et al., 2011; Lim and Hong 2012; Tao et al., 2012). Beijing-Tianjin-Hebei (BTH) region
77 is the heaviest aerosol polluted area in China and concerns have been raised about the
78 aerosol-radiation-cloud-precipitation interaction over this region. The impact of aerosols on light rainfall or
79 warm-rain processes over BTH region almost reaches consistent agreement (e.g., Qian et al., 2009), but
80 aerosol effects on the heavy convective rainfall in this region still have large uncertainties (Guo et al., 2014;
81 Wang et al., 2016).

82 The clouds that can generate heavy convective rainfall in BTH region usually contain warm clouds, cold
83 clouds and mixed-phase clouds (e.g. Guo et al., 2015). Because the aerosol-cloud interactions in different

思媛 周 19/7/21 12:02 AM

已删除: carbons

思媛 周 19/7/21 12:02 AM

已删除: sulfates

思媛 周 19/7/21 12:02 AM

已删除: found. However, changes in cloud microphysics show different responses between AOD and CDNC analyses. While decreases in ice cloud effective radius are found in both analyses, the

思媛 周 19/7/21 12:02 AM

已删除: in AOD analysis but

思媛 周 19/7/21 12:02 AM

已删除: in

思媛 周 19/7/21 12:02 AM

已删除: analysis

思媛 周 19/7/21 12:02 AM

已删除: moisture (specific

思媛 周 19/7/21 12:02 AM

已设置格式: 字体:10.5 pt, 字体颜色: 文字 1

思媛 周 19/7/21 12:02 AM

已删除: at 850 hPa) on heavy rainfall and clouds was also studied and more moisture tends to increase rainfall duration.

思媛 周 19/7/21 12:02 AM

已设置格式: 字体:10.5 pt, 字体颜色: 文字 1

思媛 周 19/7/21 12:02 AM

已删除: Wang et al., 2009;

99 | types of clouds are distinct (Gryspeerd et al., 2014b), aerosol indirect effect during heavy rainfall is more
100 complicated than its direct effect (Sassen et al., 1995; Sherwood, 2002; Jiang et al., 2008, Tao et al., 2012).
101 For warm clouds, by serving as CCN that nucleates more cloud droplets, aerosols can increase cloud albedo so
102 called albedo effect or Twomey effect (Twomey, 1977), lengthen the cloud lifetime so called lifetime effect
103 (Albrecht, 1989), and enhance thin cloud thermal emissivity so called thermal emissivity effect (Garrett and
104 Zhao, 2006). The above effects tend to increase the cloud microphysical stability and suppress warm-rain
105 processes (Albrecht 1989; Rosenfeld et al. 2014). For cold clouds and mixed-phase clouds, many studies
106 reported that the cloud liquid accumulated by aerosols is converted to ice hydrometeors above the freezing
107 level, which invigorates deep convective clouds and intensifies heavy precipitation so called invigoration
108 effect (Rosenfeld and Woodley, 2000; Rosenfeld et al., 2008; Lee et al. 2009; Guo et al. 2014). The Twomey
109 effect infers that aerosols serving as CCN that increase the cloud droplets could reduce cloud droplet size
110 within a constant liquid water path (Twomey, 1977). However, the opposite results of relationship between
111 aerosols and cloud droplet effective radius were reported in observations (Yuan et al., 2008; Panicker et al.,
112 2010; Jung et al., 2013; Harikishan et al., 2016; Qiu et al., 2017), which might be related with the moisture
113 supply near the cloud base (Yuan et al., 2008; Qiu et al., 2017). Besides, the influence of aerosols on ice
114 clouds also depends upon the amount of moisture supply (Jiang et al., 2008). Therefore, how the aerosols
115 modify the heavy convective rainfall and concurrent cloud changes does not reach a consensus, particularly if
116 considering the different moisture conditions.

117 Heavy convective rainfall over BTH region usually occurs within a few hours, thus studying on the
118 relationship between aerosols and rainfall diurnal variation could deepen our understanding of aerosol effects
119 on heavy rainfall. Several previous studies have found that aerosols are related to the changes of the rainfall
120 diurnal variation in other regions (Kim et al., 2010; Gryspeerd et al., 2014b; Fan et al., 2015; Guo et al., 2016;
121 Lee et al., 2016). However, the above studies do not address the change of cloud properties and its sensitivity
122 to different conditions of moisture supply. Although our recent work over BTH region (Zhou et al. 2018)
123 attempted to remove the meteorological effect including circulation and moisture and found that the peak of
124 heavy rainfall shifts earlier on the polluted condition, it only excluded the extreme moisture conditions and
125 focused on aerosol radiative effect on the rainfall diurnal variation. Therefore, this study aims to deepen the
126 previous study (Zhou et al., 2018) through investigating the following questions: (1) how do aerosols
127 (including absorbing aerosols and scattering aerosols) modify the behaviors of the heavy rainfall diurnal
128 variation (start time, peak time, duration and intensity)? (2) how do aerosols influence the concurrent cloud
129 properties with inclusion of moisture? To solve above questions, we used aerosol optical depth (AOD) as a
130 macro indicator of aerosol pollution and cloud droplet number concentration (CDNC) as a micro indicator of
131 CCN served by aerosols respectively to compare the characteristics of heavy rainfall diurnal variation and the
132 concurrent cloud properties between clean and polluted conditions, and applied aerosol index (AI) to
133 distinguish the associated different effects of absorbing aerosols and scattering aerosols. In addition, we used
134 the specific humidity (SH) at 850 hPa as an indicator of moisture supply condition to investigate the possible

思媛 周 19/7/21 12:02 AM
已删除: 2014

思媛 周 19/7/21 12:02 AM
已删除: 2014

137 effects of moisture on the rainfall and clouds and compared them with the effects of aerosols. The paper is
138 organized as following: The data and methodology are introduced in Sect. 2. Section 3 addresses the
139 relationship between aerosol pollution and diurnal variation of heavy rainfall, including the distinct
140 characteristics of rainfall diurnal variation on clean/polluted conditions; the different behaviors of heavy
141 rainfall diurnal variation along with the change of two different types of aerosols, and the comparison of
142 heavy rainfall behaviors influenced respectively by moisture and aerosols. Section 4 describes the concurrent
143 changes of cloud properties associated with pollution and examines the **possible** influences of CCN and
144 moisture on the cloud properties. Section 5 makes a discussion on the distinct roles of aerosol radiative
145 effect/cloud effect on the behaviors of heavy rainfall diurnal variation, as well as the uncertainties of different
146 indicators and associated distinct results. Conclusion will be given in Sect. 6.

147

148 **2. Data and methodology**

149 **2.1 Data**

150 Four types of datasets from the year 2002 to 2012 (11 years) are used in this study, which include (1)
151 precipitation, (2) aerosols, (3) clouds, and (4) other meteorological fields.

152 **2.1.1 Precipitation data**

153 To study the diurnal variation of heavy rainfall, the gauge-based hourly precipitation datasets are used, which
154 were obtained from the National Meteorological Information Center (NMIC) of the China Meteorological
155 Administration (CMA) (Yu et al., 2007) at 2420 stations in China from 1951 to 2012. The quality control
156 made by CMA/NMIC includes the check for extreme values (the value exceeding the monthly maximum in
157 daily precipitation was rejected), the internal consistency check (wiping off the erroneous records caused by
158 incorrect units, reading, or coding) and spatial consistency check (comparing the time series of hourly
159 precipitation with nearby stations) [Shen et al., 2010]. Here we chose 176 stations in the plain area of BTH
160 region that are below the topography of 100 meter above sea level as shown in Fig.1, because we purposely
161 removed the probable orographic influence on the rainfall diurnal variation, which is consistent with our
162 previous work (Zhou et al., 2018). The record analyzed here is the period of 2002 to 2012.

163 **2.1.2 Aerosol data**

164 AOD is a proxy for the optical amount of aerosol particles in a column of the atmosphere and serves as one of
165 indicators for the division of aerosol pollution condition in this study, which was obtained from MODIS
166 (Moderate Resolution Imaging Spectroradiometer) Collection 6 L3 aerosol product with the horizontal
167 resolution of $1^{\circ} \times 1^{\circ}$ onboard the Terra satellite (Tao et al., 2015). The quality assurance of marginal or higher
168 confidence is used in this study. The reported uncertainty in MODIS AOD data is on the order of $(-0.02-10\%)$,
169 $(+0.04+10\%)$ (Levy et al., 2013). The Terra satellite overpass time at the equator is around 10:30 local solar

170 time (LST) in the daytime, and the satellite data is almost missing when it is rainy during the overpass time.
171 As shown in Fig.2, the occurrence of selected heavy rainfall events in this study is mainly later than the
172 satellite overpass time. Therefore, the AOD used here represents the situation of the air quality in advance of
173 heavy rainfall appearance.

174 The ultraviolet AI from Ozone Monitoring Instrument (OMI) on board the Aura satellite which was
175 launched in July 2004, is used for detecting the different types of aerosols in this study. The OMI ultraviolet
176 AI is a method of detecting absorbing aerosols from satellite measurements in the near-ultraviolet wavelength
177 region (Torres et al., 1998). The positive values of ultraviolet AI are attributed to the absorbing aerosols such
178 as smoke and dust while the negative values of AI stand for the non-absorbing aerosols (scattering aerosols)
179 such as sulfate and sea salt (Tariq and Ali, 2015). The near-zero values of AI occur when clouds and Rayleigh
180 scattering dominate (Hammer et al., 2018). The horizontal resolution of AI data is $1^{\circ}\times 1^{\circ}$ and it covers the
181 period of 2005 to 2012.

182 MACC-II (Monitoring Atmospheric Composition and Climate Interim Implementation) reanalysis product
183 produced by ECMWF (the European Centre for Medium-Range Weather Forecasts), provided the AOD
184 datasets for different kinds of aerosols (BC, sulfate, organic matter, mineral dust and sea salt). MACC-II
185 reanalysis products are observationally-based within a model framework, which can offer a more complete
186 temporal and spatial coverage than observation and reduce the shortcomings of simulation that fail in
187 simulating the complexity of real aerosol distributions (Benedetti *et al.*, 2009). The horizontal resolution of
188 MACC-II is also $1^{\circ}\times 1^{\circ}$ with the time interval of six-hour. MACC-II data covers the period of 2003 to 2012.

189 2.1.3 Cloud data

190 Daily cloud variables, including cloud fraction (CF), cloud top pressure (CTP), cloud optical thickness (COT,
191 liquid and ice), cloud water path (CWP, liquid and ice) and cloud effective radius (CER, liquid and ice), were
192 obtained from MODIS Collection 6 L3 cloud product onboard the Terra satellite. The MODIS cloud product
193 combines infrared emission and solar reflectance techniques to determine both physical and radiative cloud
194 properties (Platnick et al., 2017). The validation of cloud top properties in this product has been conducted
195 through comparisons with CALIOP (Cloud-Aerosol Lidar with Orthogonal Polarization) data and other lidar
196 observations (Holz et al., 2008; Menzel et al., 2008), and the validation and quality control of cloud optical
197 products is performed primarily using in situ measurements obtained during field campaigns as well as the
198 MODIS Airborne Simulator instrument (<https://modis-atmos.gsfc.nasa.gov/products/cloud>). Consistent with
199 AOD, the measure of above cloud variables is before the occurrence of heavy rainfall.

200 CDNC is retrieved as the proxy for CCN and also another indicator for separating different aerosol
201 conditions in this study. Currently, most derivations of CDNC assume that the clouds are adiabatic and
202 horizontally homogeneous; CDNC is constant throughout the cloud's vertical extent, and cloud liquid water

203 content varies linearly with altitude adiabatically (Min et al., 2012; Bennartz and Rausch, 2017). According to
204 Boers et al. (2006) and Bennartz (2007), we calculated CDNC (unit: cm^{-3}) through:

$$205 \quad \text{CDNC} = \frac{C_w^{1/2}}{k} \frac{10^{1/2}}{4\pi\rho_w^{1/2}} \frac{\tau^{1/2}}{R_e^{5/2}} \quad (1)$$

206 Where C_w is the moist adiabatic condensate coefficient, and its value depends slightly on the temperature
207 of the cloud layer, ranging from 1 to $2.5 \times 10^{-3} \text{ gm}^{-4}$ for a temperature between 0 °C and 40 °C (Brennguier,
208 1991). In this study, we calculated the C_w through the function of the temperature (see Fig.1 in Zhu et al.,
209 2018) at a given pressure that is 850 hPa. And we have tested the sensitivity of CDNC to the amount of C_w
210 and found it almost keeps the same when the C_w changes from 1 to $2.5 \times 10^{-3} \text{ gm}^{-4}$. The coefficient k is the
211 ratio between the volume mean radius and the effective radius and varies between 0.5 and 1 (Brennguier et al.,
212 2000). Here we used $k = 1$ for that we cannot get the accurate value of k and the value of k does not influence
213 the rank of CDNC for the division of aerosol condition in this study. ρ_w is cloud water density. τ and Re are
214 the liquid COT and CER obtained from MODIS Collection 6 L3 cloud product onboard the Terra satellite
215 with resolution of $1^\circ \times 1^\circ$. To reduce the uncertainty of CDNC retrieval caused by the heterogeneity effect from
216 thin clouds (Nakajima and King, 1990; Quaas et al., 2008; Grandey and Stier, 2010; Grosvenor et al., 2018),
217 we selected the CF more than 80%, the liquid COT more than 4 and the liquid CER more than $4 \mu\text{m}$ when
218 calculating the CDNC (Quaas et al., 2008).

219 2.1.4 Other meteorological data

220 Other meteorological factors, including wind, temperature, pressure and SH, were obtained from the
221 ERA-Interim reanalysis datasets with $1^\circ \times 1^\circ$ horizontal resolution and 37 vertical levels at six-hour intervals.
222 ERA-Interim is a global atmospheric reanalysis produced by ECMWF, which covers the period from 1979 to
223 near-real time (Dee et al., 2011). The SH, which stands for the water vapor content, serves as the indicator of
224 moisture supply condition in this study.

225

226 2.2 Methodology

227 2.2.1 Method of interpolation

228 We used both station data of gauge-based precipitation and gridded data including aerosols, clouds and other
229 meteorological variables. Gridded datasets in this study were downloaded with the horizontal resolution of
230 $1^\circ \times 1^\circ$, which are consistent with the resolution of MODIS L3 product. To unify the datasets, we interpolated
231 all the gridded datasets onto the selected 176 rainfall stations using the average value in a $1^\circ \times 1^\circ$ grid as the
232 background condition of each rainfall station, i.e., the stations in the same $1^\circ \times 1^\circ$ grid have the same aerosol,
233 cloud and meteorological conditions.

234 2.2.2 Selection of sub-season and circulation

思媛 周 19/7/21 12:02 AM

已删除:.

思媛 周 19/7/21 12:02 AM

已删除: COD

237 Consistent with our previous work, we focused on early summer (1 June to 20 July) before the large-scale
238 rainy season starts, in order to remove the large-scale circulation influence and identify the effect of aerosols on
239 local convective precipitation because BTH rainfall during this period is mostly convective rainfall (Yu et al.,
240 2007) with heavy pollution (Zhou et al., 2018). And to unify the background atmospheric circulation, we only
241 selected the rainfall days with southwesterly flow, which is the dominant circulation accounting for 40% of
242 total circulation patterns over the BTH region during early summer (Zhou et al., 2018).

243 2.2.3 Classification of the heavy rainfall, clean/polluted and moisture conditions

244 With the circulation of southwesterly, we selected heavy rainfall days when the hourly precipitation amount is
245 more than 8.0 mm/hour (defined by *Atmospheric Sciences Thesaurus, 1994*). Here “a day” is counted from 8
246 LST to 8 LST next day (0 UTC to 24 UTC). We used two indicators to distinguish the clean and polluted
247 conditions, which are AOD and CDNC. The 25th and 75th percentiles of AOD/CDNC of the whole rainfall
248 days are used as the thresholds of clean and pollution condition, and the values are shown in Tab.1. It shows
249 that there are 514 cases of heavy rainfall on polluted days and 406 cases of that on clean days when using
250 AOD, and 630/716 cases on polluted/clean condition when using CDNC.

251 The absorbing aerosols are detected using the positive values of AI that is named as absorbing aerosol index
252 (AAI) here, and we can retrieve the scattering aerosol index (SAI) using the negative values of AI. AAI and
253 SAI are also divided into two groups using the threshold of 25th/75th percentile as shown in Tab.1. We used
254 AAI/SAI more than 75th as the extreme circumstances of absorbing/scattering aerosols to compare their
255 impacts on heavy rainfall. The case numbers are 375 and 550 respectively for the extreme AAI and SAI cases.
256 Using the same method, we chose cases with more BC/sulfate when the AOD of BC/sulfate is larger than the
257 75th percentile of itself in all rainy days, and cases with less BC/sulfate when that is less than the 25th
258 percentile of itself in the same situation. Accordingly, we selected 459 heavy rainfall cases with more BC and
259 274 cases with less BC. Similarly, 361 cases with more sulfate and 419 cases with less sulfate with heavy
260 rainfall were selected.

261 The SH at 850 hPa is used as the indicator of moisture supply under the cloud base. We chose wet cases
262 when the SH on that day is larger than 75th percentile of the whole rainy days, and chose dry cases when SH
263 on that day is less than the 25th percentile of the whole rainy days (the thresholds are shown in Tab. 1).

264 2.2.4 Statistical analysis

265 We adopted the probability distribution function (PDF) to compare the features of heavy rainfall and cloud
266 variables on different conditions of aerosols, through which we can understand the changes of rainfall/cloud
267 properties more comprehensively. The numbers of bins we selected in the study have been all tested for better
268 representing the PDF distribution. Student's t-test is used to examine the significance level of differences
269 between the different groups of aerosol conditions.

270

思媛 周 19/7/21 12:02 AM
已删除: aerosols and

思媛 周 19/7/21 12:02 AM
已删除: condition

思媛 周 19/7/21 12:02 AM
已删除: with heavy rainfall

思媛 周 19/7/21 12:02 AM
已删除: rainy

思媛 周 19/7/21 12:02 AM
已删除: tercile

思媛 周 19/7/21 12:02 AM
已删除: tercile

277 **3. Relationship between aerosol pollution and diurnal variation of heavy rainfall over BTH**

278 **3.1 Distinct characteristics of heavy rainfall diurnal variation associated with aerosol pollution**

279 Our previous study (Zhou et al. 2018) has reported the distinct peak shifts of rainfall diurnal variation between
280 clean and polluted days using the indicator of AOD over the BTH region during early summer. Similar with
281 our previous study, the PDF of the heavy rainfall peak time shows that the maximum of rainfall peak is about
282 two hours earlier on the polluted days (20:00 LST) than that on the clean days (22:00 LST) (Fig. 2a). To
283 comprehensively recognize the changes of rainfall diurnal variation associated with air qualities, here we
284 examined the PDF of the start time, the duration and the intensity besides the peak time of heavy rainfall.

285 As shown in Fig. 2a, the start time of heavy rainfall exhibits a significant advance on the polluted days. The
286 secondary peak on the early morning is ignored here because the early-morning rainfall is usually associated
287 with the mountain winds (Wolyn et al., 1994; Li et al., 2016) and the nighttime low-level jet (Higgins et al., 1997;
288 Liu et al., 2012) that is beyond the scope of this study. The time for the maximum frequency of heavy rainfall
289 initiation is around 6 hours earlier on the polluted days, shifting from around 0:00 LST on the clean days to
290 the 18:00 LST (Fig. 2a). Regarding the rainfall durations, the average persistence of heavy rainfall on polluted
291 days is 0.8 hours longer than that on clean days (Tab. 2). According to the PDF shown as in Fig. 2a, the
292 occurrence of short-term precipitation (≤ 6 hours, Yuan et al., 2010) decreases while that of long-term
293 precipitation (>6 hours, Yuan et al., 2010) increases. The intensity of hourly rainfall exhibits a non-significant
294 increase on the polluted days.

295 The distinct behaviors of heavy rainfall diurnal variation between clean and polluted days have been well
296 demonstrated using the indicator of AOD. However, AOD is not a proper proxy for CCN (Shinozuka et al.,
297 2015) but the property of aerosols serving as CCN should be considered because aerosol-cloud interaction
298 plays an indispensable role on changing rainfall diurnal variation. Therefore, here we applied the retrieved
299 CDNC as the indicator of CCN (Zeng et al., 2014; Zhu et al., 2018) to examine the above-mentioned results.
300 As a result, the similar changes of heavy rainfall can be well exhibited in CDNC analysis as shown in Fig. 2b.
301 The start time and peak time of heavy rainfall on the polluted condition also show significant advances
302 compared with that on the clean condition, with the average advances of 1.4 hours and 3.0 hours respectively
303 (Tab. 2). The duration of heavy rainfall on the polluted condition is also prolonged, which is 2.2 hours longer
304 in average (Tab. 2). Similar with the results based on AOD, the difference of rainfall intensity between clean
305 and polluted conditions using CDNC does not pass the 95% statistical confidence level as well.

306 Hence, the results using either AOD or CDNC show that the start and peak time of heavy rainfall occur
307 earlier and the duration becomes longer under pollution, although there are some quantitative differences
308 between the two indicators. Since the difference of rainfall intensity is not significant in this study, the
309 following analysis only focuses on studying the start time, peak time and duration of heavy rainfall along with
310 aerosol pollution.

思媛 周 19/7/21 12:02 AM
已设置格式: 字体:Times

311

312 **3.2 Distinct behaviors of heavy rainfall diurnal variation associated with two different types of aerosols**

313 Using the indicator of AI, we further investigated the distinct behaviors of heavy rainfall diurnal variation
 314 related to absorbing aerosols and scattering aerosols respectively. The PDF of start time, peak time and
 315 duration of heavy rainfall under the extreme circumstances of absorbing aerosols and scattering aerosols are
 316 compared in Fig. 3. Here, we briefly named the days with extreme large amount of absorbing aerosols as
 317 absorbing aerosol days and with more scattering aerosols as scattering aerosol days. The start time of heavy
 318 rainfall on absorbing aerosol days shows a significant earlier compared with that on scattering aerosol days
 319 (Fig. 3a), with 0.7 hours advance in average (Tab. 3). Similarly, the rainfall peak time also shows earlier on
 320 absorbing aerosol days (Fig. 3b), with an average advance of 1.6 hours (Tab. 3). The rainfall duration on
 321 scattering aerosol days shows longer than that on absorbing aerosol days, which are 6.0 hours and 5.0 hours
 322 respectively in average (Tab. 3). All the above-mentioned differences between the two groups have passed 95%
 323 statistical confidence level. The results indicate that the absorbing aerosols and scattering aerosols may have
 324 different or inverse effects on the heavy rainfall that absorbing aerosols may generate the heavy rainfall in
 325 advance while the scattering aerosols may delay and prolong the heavy rainfall.

326 To further verify the different behaviors of heavy rainfall diurnal variation associated with two different
 327 types of aerosols, we purposely re-examine the above-mentioned phenomena using BC/sulfate that can
 328 represent typical absorbing/scattering aerosols over the BTH region. BC has its maximum center over BTH
 329 region (Fig. 4a) and our previous study has indicated that the radiative effect of BC low-level warming may
 330 facilitate the convective rainfall generation (Zhou et al., 2018). The percentage of sulfate is also large over the
 331 BTH region (Fig. 4b) and the sulfate is one of the most effective CCN that influences the precipitation in this
 332 region (Gunthe et al., 2011). Accordingly, we selected the cases with different amounts of BC and sulfate
 333 AOD to compare their roles on the diurnal variation of heavy rainfall. The methods have been described in
 334 Sect. 2.2.3. The PDF of the start time, peak time and duration of heavy rainfall in the cases with more/less
 335 amount of BC are shown in Fig. 5a, respectively. The most striking result is that the maximum frequency of
 336 rainfall start time in the more BC cases evidently shifts earlier (Fig. 5a). Meanwhile, the mean peak time in
 337 the more BC cases shows 1.1 hour earlier than that in the less BC cases (Tab. 3). And the duration of heavy
 338 rainfall is slightly shortened by the averaged 0.2 hours in the more BC cases. The features in more BC cases
 339 are consistent with the above results of absorbing aerosols. In contrast, when the sulfate has higher amount,
 340 the mean start time of rainfall is delayed by 0.5 hours, while the duration shows a significant increase by 1.5
 341 hours in average (Tab. 3). The behaviors in the more sulfate cases also exhibit similar with the above results
 342 of scattering aerosols, except for the peak time that shows later in the scattering aerosol cases but a little
 343 earlier in the more sulfate cases (Tab. 3).

344

思媛 周 19/7/21 12:02 AM
 已删除: higher and lower
 思媛 周 19/7/21 12:02 AM
 已删除: high
 思媛 周 19/7/21 12:02 AM
 已删除: high
 思媛 周 19/7/21 12:02 AM
 已删除: low
 思媛 周 19/7/21 12:02 AM
 已删除: high
 思媛 周 19/7/21 12:02 AM
 已删除: high
 思媛 周 19/7/21 12:02 AM
 已删除: aerosol effect
 思媛 周 19/7/21 12:02 AM
 已删除: high
 思媛 周 19/7/21 12:02 AM
 已删除: aerosol effect
 思媛 周 19/7/21 12:02 AM
 已删除: aerosols
 思媛 周 19/7/21 12:02 AM
 已删除: high

356 **3.3 Behavior comparisons of heavy rainfall diurnal variation influenced by moisture and aerosol.**

357 Moisture supply is an indispensable factor for the precipitation formation. Since the southwesterly circulation
358 can not only transport pollutants but also plenty of moisture to the BTH region (Wu et al., 2017), more
359 pollution usually corresponds to more moisture for the BTH region (Sun et al., 2015) so that it is hard to
360 completely remove the moisture effect on the above results in the pure observational study. Here we attempt
361 to recognize the moisture effect on the heavy rainfall to further understand the above aerosol-associated
362 changes. Because the moisture supply for BTH is mainly transported via low-level southwesterly circulation,
363 we purposely used the SH at 850 hPa as the indicator of moisture condition.

364 Using the similar percentile method with polluted/clean days, we got the rainfall characteristics in the more
365 humid (more than 75th percentile) and the less humid (less than 25th percentile) environments on the heavy
366 rainfall days regardless of the aerosol condition, as shown in Fig. 6a. The results show that the start time of
367 heavy rainfall is delayed by 0.9 hours, the peak time is 0.6 hours earlier and the duration is prolonged by 2.0
368 hours in average in the more humid environment, which is similar with the results of the more sulfate cases.
369 Besides, the same results are obtained with different moisture indicator, e.g. the 850 hPa absolute humidity.
370 These results indicate the advance of heavy rainfall start time on the polluted days is not caused by more
371 moisture supply, while the longer duration and earlier peak in the more sulfate cases might be related to the
372 increased moisture supply.

373 We also investigate the distributions of moisture and rainfall behaviors in the clean and polluted cases
374 respectively using AOD and CDNC (Fig. 6 b&c). The results show that the relationship between moisture and
375 rainfall start time/peak time/duration is not linear. Using either AOD or CDNC, the distribution of SH exhibits
376 a slight increase in the polluted cases, indicating that the polluted cases have the more moisture than the clean
377 cases which is particularly well shown using AOD. However, when fixing the moisture at a certain range
378 especially at the relative dry condition, we can detect the similar phenomena of earlier start/peak time and
379 longer duration in the polluted cases. For example, when the amount of 850 hPa SH is between 8-12 g/kg, the
380 start & peak time in the polluted cases show significant earlier and the duration exhibits slightly increased
381 compared with that in the clean cases using either AOD or CDNC.

382 The above results indicate that the advance of heavy rainfall start and peak time in the polluted cases might
383 be weakly related to the moisture effect, but the moisture could obviously prolong the duration of heavy
384 rainfall (Fig. 6a). Because the diurnal change of heavy rainfall with more moisture is similar with the
385 behaviors of heavy rainfall with scattering aerosols especially sulfate, we cannot figure out their individual
386 role at present.

387
388 **4 Relationship between aerosol pollution and concurrent changes of cloud properties associated with**
389 **heavy rainfall diurnal variation**

- 思媛 周 19/7/21 12:02 AM
已删除: tercile
- 思媛 周 19/7/21 12:02 AM
已删除: tercile
- 思媛 周 19/7/21 12:02 AM
已删除: hour
- 思媛 周 19/7/21 12:02 AM
已删除: result on
- 思媛 周 19/7/21 12:02 AM
已删除: condition of
- 思媛 周 19/7/21 12:02 AM
已删除: high
- 思媛 周 19/7/21 12:02 AM
已删除: characteristics
- 思媛 周 19/7/21 12:02 AM
已删除: low-level
- 思媛 周 19/7/21 12:02 AM
已删除: behavior distribution

思媛 周 19/7/21 12:02 AM
已删除: in this section

400 **4.1 Concurrent changes of cloud properties along with heavy rainfall diurnal variation on clean and**
401 **polluted conditions**

402 To understand the cloud effect of aerosols during heavy rainfall diurnal variation, we need to recognize the
403 concurrent cloud characteristics on the clean and polluted conditions. The cloud properties we used were
404 obtained from satellite product that were measured at the same time with aerosols before the occurrence of
405 heavy rainfall. The differences of cloud features were examined in both macroscopic (including CF, CTP,
406 COT and CWP) and microscopic properties (including CER) between the clean and polluted conditions based
407 on AOD and CDNC respectively, as shown in Fig. 7.

408 Using AOD as the pollution indicator, the PDF distribution of CF shows that the CF on the polluted
409 condition is evidently larger than that on the clean condition. The average CF is 62.8% on the clean condition,
410 and 89.3% on the polluted condition, (Tab. 4), which is increased by 26.1%. The average CTP on the polluted
411 condition is 487.3 hPa, which is larger than 442.3 hPa on the clean condition and increases 45 hPa, indicating
412 that the cloud top height is lower on the polluted days. The COT, CWP and CER were further analyzed for the
413 liquid and ice portions of clouds as shown in Fig. 7. Both liquid and ice COT on polluted condition exhibit
414 significant increases compared with that on clean condition. The mean amount of liquid COT is increased by
415 3.1 and ice COT increases by 6.2 (Tab. 4). Similar with COT, the amount of liquid and ice CWP also increase
416 on polluted condition, which increase by 33.6 g/m² and 88.2 g/m² respectively. In addition, the liquid CER is
417 increased by 0.8 μm and the ice CER is decreased by 2.8 μm on the polluted days. The differences of above
418 cloud properties between clean and polluted cases have all passed the 95% statistical confidence level.

419 Using CDNC as another pollution indicator, the above-mentioned changes of cloud properties are consistent
420 with that using AOD, except for liquid CER (Fig. 7). Since the calculation method of CDNC is not
421 independent on the liquid COT and liquid CER, we would not directly compare the results of liquid COT and
422 CER based on CDNC with those based on AOD here. But according to other variables that are independent of
423 the CDNC calculation, we found the cases with more CDNC are accompanied with the increase of CTP, ice
424 COT and liquid & ice CWP, which increase by 32.8 hPa, 24.4, 215.8 g/m² and 370.9 g/m² respectively (Tab 4)
425 and all of which are consistent with the results based on AOD. The CER of ice clouds also shows a consistent
426 decrease by 8.8 μm on the polluted condition based on CDNC. We noticed that the changes of the
427 COT/CWP/CER for both liquid and ice based on CDNC are much larger than that based on AOD, which
428 indicates that these cloud properties might be more sensitive to the indicator of CDNC rather than AOD.

429 According to the above comparison, the concurrent changes of cloud properties along with heavy rainfall
430 diurnal variation show consistent results using the two pollution indicators (AOD and CDNC). The pollution
431 corresponds to the increase of CF, ice COT, liquid and ice CWP, but the decrease of cloud top height (the
432 increase of CTP corresponds to the decrease of cloud top height) and ice CER. With the increase of AOD,
433 both the liquid COT and liquid CER are increased. Since we cannot distinguish the liquid part of mix-phased
434 clouds from liquid (warm) clouds in the observation, the changes of liquid cloud properties above might come

- 思媛周 19/7/21 12:02 AM
已删除: , which increases 42.2%
- 思媛周 19/7/21 12:02 AM
已删除:).
- 思媛周 19/7/21 12:02 AM
已删除: 10.2%,
- 思媛周 19/7/21 12:02 AM
已删除: 44.9%
- 思媛周 19/7/21 12:02 AM
已删除: 92.5%
- 思媛周 19/7/21 12:02 AM
已删除: 53.5%
- 思媛周 19/7/21 12:02 AM
已删除: 71.6%
- 思媛周 19/7/21 12:02 AM
已删除: 4
- 思媛周 19/7/21 12:02 AM
已删除: %
- 思媛周 19/7/21 12:02 AM
已删除: .8%
- 思媛周 19/7/21 12:02 AM
已删除: The PDF of liquid CER on the polluted condition shifts to larger size based on AOD but smaller size based on CDNC. The inconsistency of liquid CER using two indicators might be due to
- 思媛周 19/7/21 12:02 AM
已删除: which
- 思媛周 19/7/21 12:02 AM
已删除: CF,
- 思媛周 19/7/21 12:02 AM
已删除: COD
- 思媛周 19/7/21 12:02 AM
已删除: .2%, 280.5%, 210.7%
- 思媛周 19/7/21 12:02 AM
已删除: 216.1%
- 思媛周 19/7/21 12:02 AM
已删除: 25.7%
- 思媛周 19/7/21 12:02 AM
已删除: and CWP both for
- 思媛周 19/7/21 12:02 AM
已删除: The changes of liquid CER are opposite between the two indicators, but it might be due to the potential negative correlation between liquid CER and CDNC in the CDNC retrieval.

462 from both the liquid (warm) clouds and the liquid part of mixed-phase clouds. Likewise, the above-mentioned
463 changes of ice cloud properties might come from both ice (cold) clouds and the ice part of mixed-phase
464 clouds.

465

466 | 4.2 Influences of CDNC (CCN) and moisture on the cloud properties

467 Section 3.3 has shown that the diurnal variation of heavy rainfall with more moisture supply is similar with
468 the changes of heavy rainfall with more sulfate aerosol. We assume that the moisture under the cloud base and
469 the sulfate serving as CCN both influence the cloud properties (Yuan et al., 2008; Jiang et al., 2008; Jung et al.,
470 2013; Qiu et al., 2017). To identify the effect of aerosols on clouds and its sensitivity to moisture, we
471 purposely investigated the changes of above cloud properties with different conditions of the CDNC and the
472 low-level moisture (850hPa SH) respectively. We categorized all cases of heavy rainfall into four groups,
473 which are (1) clean and dry, (2) polluted and dry, (3) clean and wet, (4) polluted and wet, and checked the
474 changes of above cloud properties, as shown in Tab. 5. To retrieve the comparable samples, here
475 “clean/polluted” refers to the CDNC on that rainfall day less/more than 25th/75th percentile of the CDNC
476 among the heavy rainfall days, and similarly, the “dry/wet” refers to the SH on that rainfall day less/more than
477 25th/75th percentile of itself among the heavy rainfall days. The average CDNC is 68.58 cm⁻³ on the dry
478 condition and 68.56 cm⁻³ on the wet condition, and the average SH is 11.3 g/kg and 11.8 g/kg on the clean and
479 polluted conditions respectively, thus we can consider the CDNC or SH remain the same when the other
480 condition changes. We made the significant test of differences between group 1 and 2, group 1 and 3, group 2
481 and 4, group 3 and 4. Because the CF is fixed above 80% when calculating the CDNC (see in Sect. 2.1.3),
482 here the selected groups all belong to the condition of higher CF.

483 Comparing the results of group 1 and 2, which are both on the dry condition, we can identify the influence
484 of CDNC on the cloud properties, which stands for the effect of CCN. The changes of these cloud variables
485 are the same as that in Sect. 4.1, that the CF, ice COT and liquid & ice CWP are increased on the polluted
486 condition, while the cloud top height and ice CER are decreased based on CDNC. Among these variables, the
487 ice COT and liquid & ice CWP are especially larger on the polluted condition, which are 5-6 times larger than
488 that on the clean condition (Tab. 5). On the wet condition, comparing the group 3 and 4, the changes are
489 similar that the CF, ice COT and liquid & ice CWP are increased and the ice CER are decreased but the
490 change of CTP becomes not significant. However, the changes of these variables on the dry condition are
491 evidently enhanced than that on the wet condition, which indicates these cloud properties might be more
492 sensitive to CDNC on the dry condition. The above comparisons indicate that with the increase of CDNC
493 (CCN), the CF, ice COT and liquid & ice CWP are increased while the ice CER is decreased regardless of the
494 moisture amount. Although the comparisons of liquid COT and liquid CER based on CDNC are meaningless
495 since the CDNC is calculated by the two variables, we infer that the increase of liquid COT and the decrease
496 of liquid CER (Tab. 5) might be not completely caused by CDNC calculation but the natural effect of CCN.

- 思媛 周 19/7/21 12:02 AM
已删除: tercile
- 思媛 周 19/7/21 12:02 AM
已删除: tercile
- 思媛 周 19/7/21 12:02 AM
已删除: 2168.7
- 思媛 周 19/7/21 12:02 AM
已删除: 2168.1
- 思媛 周 19/7/21 12:02 AM
已删除: .
- 思媛 周 19/7/21 12:02 AM
已删除: 5
- 思媛 周 19/7/21 12:02 AM
已删除: CWP both for
- 思媛 周 19/7/21 12:02 AM
已删除: and
- 思媛 周 19/7/21 12:02 AM
已删除: liquid &
- 思媛 周 19/7/21 12:02 AM
已删除: liquid &
- 思媛 周 19/7/21 12:02 AM
已删除: . The liquid CER on polluted condition also changes evidently, which becomes almost a half of that on clean condition.
- 思媛 周 19/7/21 12:02 AM
已删除: both for liquid and ice
- 思媛 周 19/7/21 12:02 AM
已删除: liquid and
- 思媛 周 19/7/21 12:02 AM
已删除: the
- 思媛 周 19/7/21 12:02 AM
已删除: which stands for
- 思媛 周 19/7/21 12:02 AM
已删除: for both liquid and ice clouds

516 Comparing the results of group 1 and 3, we can get the changes of cloud properties related only to moisture
517 on the same clean condition. A common feature is that CTP, COT and CWP both for liquid and ice exhibit
518 increases along with the increase of moisture. Compared with the CTP on the clean and dry condition, it
519 increases on both polluted & dry condition (group 2) and clean & wet condition (group 3), but on the former
520 condition its increase is larger, which indicates the influence of moisture on CTP might be secondary
521 compared to the CDNC (CCN) effect. Similarly, comparing the COT/CWP in group 2 and 3, the increases of
522 COT and CWP both for liquid and ice in group 2 are 3-6 times larger than that in group 3, which indicates that
523 the influences of moisture on COT and CWP may not overcome the influence of CCN. With the increase of
524 moisture, the change of liquid CER is not significant on the same clean condition, but the ice CER is
525 significantly decreased. On the polluted condition, comparing group 2 and 4, we found the COT and CWP
526 both for liquid and ice on the wet condition are evidently smaller than that on the dry condition, which
527 indicates that increasing the moisture might partly compensate for the influence of CDNC (CCN) on
528 COT/CWP.

529 The results above indicate that both CDNC (CCN) and moisture have impacts on cloud properties. They
530 both contribute to the increase of CF, COT and CWP, in which the influence of CDNC (CCN) on COT and
531 CWP are significantly larger than moisture. The increase of either CDNC or moisture corresponds to the
532 increase of CTP. But when the CDNC and moisture increase simultaneously, the CTP becomes smaller. Both
533 CDNC and moisture correspond to the significant decrease of ice CER, while only CDNC corresponds to the
534 decrease of liquid CER and that might be ascribed to the calculation method of CDNC. To reduce
535 uncertainties, we have tested the SH at different levels (e.g., 700 hPa and 800 hPa) and different moisture
536 indicator (e.g. absolute humidity) to verify above results, and found most cloud variables show the similar
537 changes with the above except for the CTP and the liquid CER, which indicates the changes of CTP and liquid
538 CER are more sensitive and have larger uncertainties. Since the behaviors of cloud changes are similar along
539 with the increase of either CDNC (CCN) or moisture but more sensitive to the former, the results in Sect. 4.1
540 might actually reflect the combined effect of CCN and moisture, and the aerosol effect on these cloud
541 properties might be dominant on the polluted days.

542

543 5. Discussion

544 5.1 Different roles of aerosol radiative effect and cloud effect in heavy rainfall

545 In Sect. 3 we found that the heavy rainfall has earlier start and peak time, and longer duration on the
546 polluted condition. And afterwards, the earlier start of rainfall under pollution was found related to absorbing
547 aerosols mainly referring to BC (Fig. 3a&5a). We also compared the effect of BC on the associated clouds.
548 Figure 8a shows the CF larger than 90% rarely occurs in the more BC environment, which might be
549 associated with the semi-direct effect of BC (Ackerman, 2000) or estimated inversion strength and BC

思媛 周 19/7/21 12:02 AM
已删除: does
思媛 周 19/7/21 12:02 AM
已删除: The
思媛 周 19/7/21 12:02 AM
已删除: with the increase of moisture.

思媛 周 19/7/21 12:02 AM
已删除: CCN
思媛 周 19/7/21 12:02 AM
已删除: CCN
思媛 周 19/7/21 12:02 AM
已删除: CCN
思媛 周 19/7/21 12:02 AM
已删除: CCN
思媛 周 19/7/21 12:02 AM
已删除: significant

思媛 周 19/7/21 12:02 AM
已删除: 5

思媛 周 19/7/21 12:02 AM
已删除: time

思媛 周 19/7/21 12:02 AM
已删除: high
思媛 周 19/7/21 12:02 AM
已删除: IPCC, 2013

562 | co-vary. This result indicates the influence of BC on the heavy rainfall in Fig. 5a is mainly due to the radiative
563 effect rather than the cloud effect. The mechanism of BC effect on the heavy rainfall can be interpreted by our
564 previous study (Zhou et al., 2018) as: BC absorbs shortwave radiation during the daytime and warms the
565 lower troposphere at around 850 hPa, and then increases the instability of the lower to middle atmosphere
566 (850-500hPa) so that enhances the local upward motion and moisture convergence. As a result, the
567 BC-induced thermodynamic instability of the atmosphere triggers the occurrence of heavy rainfall in advance.
568 Thus, the low-level heating effect of BC might play a dominant role in the beginning of rainfall especially
569 before the formation of clouds during the daytime.

思媛 周 19/7/21 12:02 AM
已删除: covary

570 | The delayed start of heavy rainfall with scattering aerosols in Fig. 3a and more sulfate in Fig. 5b is
571 consistent with many studies that both the radiative effect and cloud effect of sulfate-like aerosols could delay
572 or suppress the occurrence of rainfall (Guo et al., 2013; Wang et al., 2016; Rosenfeld et al. 2014). Sulfate-like
573 aerosols as scattering aerosols could prevent the shortwave radiation from arriving at the surface thus cool the
574 surface and stabilize the atmosphere, which suppresses the rainfall formation (Guo et al., 2013; Wang et al.,
575 2016). Sulfate-like aerosols serving as CCN can also suppress the rainfall by cloud effect through reducing the
576 cloud droplet size and thus suppressing the collision-coalescence process of cloud droplets (Albrecht 1989;
577 Rosenfeld et al. 2014). Figure 8b does shows that in contrast with BC, the CF larger than 90% is significantly
578 increased in the more sulfate environment, which indicates the sulfate-like aerosols might have more evident
579 influence on the clouds and subsequently the rainfall changes associated with sulfate are probably due to the
580 cloud effects. Another significant feature is the longer duration of heavy rainfall in both the scattering aerosol
581 cases and more sulfate cases (Fig 3c&5b). Since the heavy rainfall shows the similar changes of delayed start
582 and longer duration with the increase of sulfate and moisture, we currently cannot separate their respective
583 roles in this study. We speculate that the postponed start of heavy rainfall is mainly due to the effect of
584 sulfate-like aerosols. While the longer duration is caused by both the cloud effect of sulfate-like aerosols and
585 the increased moisture supply, because increasing either CCN or the moisture supply can increase cloud water
586 (Sect. 4.2), which could lead to the longer rainfall duration. To further investigate the mechanism of longer
587 duration, we need the assistance of numerical model simulations in the future work.

思媛 周 19/7/21 12:02 AM
已删除: higher

思媛 周 19/7/21 12:02 AM
已删除: high

思媛 周 19/7/21 12:02 AM
已删除: high

588 | Accordingly, we speculate that the earlier start time of heavy rainfall related to absorbing aerosols (BC) is
589 due to the radiative heating of absorbing aerosols, while the longer rainfall duration is probably caused by
590 both the cloud effect of sulfate-like aerosols and the increased moisture supply. As a summary we use a
591 schematic diagram (Fig. 9) to illustrate how aerosols modify the heavy rainfall over the BTH region. On one
592 hand, BC heats the lower troposphere, changing the thermodynamic condition of atmosphere, which increases
593 upward motion and accelerates the formation of cloud and rainfall. On the other hand, the increased upward
594 motion transports more sulfate-like particles and moisture into the clouds so that more CCN and sufficient
595 moisture increase the cloud water, thus might prolong the duration of rainfall. As a result, the heavy rainfall
596 over BTH region in southwesterly shows earlier start and peak time, and longer duration might due to the
597 combined effect of aerosol radiative effect, aerosol cloud effect as well as moisture effect. To further

思媛 周 19/7/21 12:02 AM
已删除: effect

603 distinguish the individual effect, we need to conduct numerical model simulations in our future study.

604

605 5.2 Uncertainties of different indicators and associated distinct results

606 The gauge-based hourly precipitation data used in this study is more reliable than other observational and
607 reanalysis precipitation data. In contrast with precipitation datasets, the observation of aerosols and clouds
608 from MODIS might have larger uncertainties, e.g., which come from the misdetection of CF when AOD is
609 large (Brennan et al., 2005; Levy et al., 2013) or the mutual interference between liquid and ice clouds (Holz
610 et al., 2008; Platnick et al., 2017).

611 In this study we used two pollution indicators, AOD and CDNC, which discriminates the pollution levels
612 for different purposes. AOD is a good proxy for the large-scale pollution level, but it stands for the optical
613 feature of aerosols and cannot well represent CCN when we studied the aerosol-cloud interaction (Shinozuka
614 et al., 2015). The value of AOD is also influenced by moisture condition, which is aerosol humidification
615 effect (Twohy et al., 2009; Altaratz et al., 2013). Therefore, we comprehensively analyzed the moisture effect
616 on the results. CDNC is a better proxy for CCN, which facilitates the study on the cloud changes associated
617 with aerosol pollution. But the retrieved CDNC has larger uncertainties. First, the assumptions in the
618 calculation of CDNC are idealized that CDNC is constant with height in a cloud and cloud liquid water
619 increases monotonically at an adiabatic environment (Grosvenor et al., 2018), but the target of this study is the
620 convective clouds with rainfall that may be not consistent with the adiabatic assumption. Second, as indicated
621 by Grosvenor et al. (2018), the uncertainties in the pixel-level retrievals of CDNC from MODIS with $1^\circ \times 1^\circ$
622 spatial resolution can be above 54%, which come from the uncertainties of parameters and the original COT
623 and CER data using in the calculation, and also the influence of heterogeneity effect from thin clouds. To
624 reduce the influence of heterogeneity effect as much as possible, we have attempted to limit the conditions of
625 CF, liquid COT and CER when calculating CDNC in the study. Besides, this study primarily focuses on the
626 relative changes of CDNC, which may be also influenced by the potential systematic biases in the CDNC
627 calculation, but actually reduced the uncertainties of absolute values.

628 We applied ultraviolet AI and AOD of BC/sulfate to identify different types of aerosols. The AI datasets
629 from OMI, which can distinguish the absorbing aerosols and scattering aerosols, also have uncertainties
630 especially for the near-zero values. Hence, we only compare the extreme circumstances of absorbing aerosols
631 and scattering aerosols. We also found the AI has a weak positive correlation with AOD from MODIS, which
632 indicates the results on absorbing aerosol days might represent the results on polluted days if identified by
633 AOD. To avoid the uncertainty, we re-examined the results using AI when removing the polluted cases
634 identified by AOD, and found the major results are not changed. The comparisons of BC/sulfate AOD cases
635 also have uncertainties because they are retrieved from MACC reanalysis data. Although the above four
636 indicators have their own uncertainties, currently we cannot find more reliable datasets in a long-term

思媛 周 19/7/21 12:02 AM
已删除:.)

思媛 周 19/7/21 12:02 AM
已删除: COD

思媛 周 19/7/21 12:02 AM
已删除: COD

思媛 周 19/7/21 12:02 AM
已删除: applied

641 observational record. The major findings using these four indices could well identify the changes of rainfall
642 and clouds accompanied with aerosols, but are insufficient to clarify the aerosol effect on clouds and
643 precipitation.

644 Using AOD and CDNC we have drawn the same conclusion that the heavy rainfall occurs in advance and
645 the duration is prolonged under pollution (Fig. 2). We found the AOD and CDNC only have a weak positive
646 correlation, which denotes that the selected cases could be different between using AOD and CDNC. The
647 cases of heavy rainfall using CDNC seem more extreme, because CDNC cases exhibit more evident changes
648 of rainfall behaviors in average than that using AOD. The quantitative difference of results between the two
649 indicators might due to the non-linear relationship of CCN and pollution that the CCN won't continuously
650 increase when aerosol loading is huge (e.g., Jiang et al., 2016), or due to the misdetection of AOD, the
651 calculation uncertainty of CDNC, and the sampling differences between AOD and CDNC. Since both the two
652 indicators have their uncertainties, we cannot say the result of which one is more reliable.

653 Most cloud properties also exhibit the consistent changes using AOD and CDNC. First, the CF and CWP
654 (liquid and ice) increase with pollution, might because the aerosols serving as CCN can nucleate a larger
655 number of cloud droplets and accumulate more liquid water in the cloud thus increase the CF and CWP.
656 Second, the CTP increases under pollution using both AOD and CDNC, which denotes the decrease of the
657 cloud top height. We speculate that the earlier start of the precipitation process could inhibit the vertical
658 growth of clouds shown as in Fig. 2. Third, the ice CER decreases under pollution using either AOD or CDNC,
659 which could be ascribed to that the increased cloud droplet number leads to more cloud droplets transforming
660 into ice crystals and causes the decrease of ice CER (Chylek et al., 2006; Zhao et al., 2018; Gryspeerd et al.,
661 2018). Currently the detailed physical processes of cold clouds and mixed-phase clouds are not clear,
662 including the diffusional grow, accretion, riming and melting process of ice precipitation (Cheng et al., 2010),
663 which needs numerical model simulations to be further explored.

664 However, the results of liquid CER might have more uncertainties. The liquid CER is increased when AOD
665 increases (Fig. 7), which might be related to the aerosol humidification effect, the misdetection of AOD and
666 cloud water, and also might result from the earlier formation of the clouds and heavy rainfall on the polluted
667 days. In addition, the relationships between satellite AOD and some cloud properties have been shown to be
668 affected by meteorological co-variations, e.g., high humid could lead to strong positive relationship of AOD
669 and CF (Quaas et al., 2010; Grandey et al., 2013) and the relationship of AOD and CTP could be also affected
670 by meteorology (Gryspeerd et al., 2014a), which indicates that the changes of cloud properties in this study
671 might be influenced by the meteorological co-variations rather than the aerosol effect. Although we have
672 considered the influence of moisture on the precipitation and clouds, the moisture variables cannot completely
673 represent all the meteorological co-variations between aerosol and precipitation (Boucher and Quaas, 2012).

674

思媛周 19/7/21 12:02 AM
已删除: , and the
思媛周 19/7/21 12:02 AM
已删除: can be well shown in

思媛周 19/7/21 12:02 AM
已删除: cases selected by

思媛周 19/7/21 12:02 AM
已删除: and

思媛周 19/7/21 12:02 AM
已删除: CDNC

思媛周 19/7/21 12:02 AM
已删除: AOD

思媛周 19/7/21 12:02 AM
已删除: , COT

思媛周 19/7/21 12:02 AM
已删除: both for

思媛周 19/7/21 12:02 AM
已删除: clouds

思媛周 19/7/21 12:02 AM
已删除: , COT

思媛周 19/7/21 12:02 AM
已删除: both

思媛周 19/7/21 12:02 AM
已删除: and

思媛周 19/7/21 12:02 AM
已删除: different result occurs for

思媛周 19/7/21 12:02 AM
已设置格式: 字体颜色: 黑色

思媛周 19/7/21 12:02 AM
已删除: between using AOD and using CDNC.

思媛周 19/7/21 12:02 AM
已设置格式: 字体颜色: 黑色

思媛周 19/7/21 12:02 AM
已删除: decreased when CDNC increases but

思媛周 19/7/21 12:02 AM
已删除: 7). The former is actually the natural result of the negative relationship between CDNC and liquid CER in the calculation. And the latter

思媛周 19/7/21 12:02 AM
已删除: Therefore, the changes of liquid CER with pollution have some uncertainties.

697 **6. Conclusions**

698 Using the gauge-based hourly rainfall records, aerosol and cloud satellite products and high temporal
699 resolution reanalysis datasets during 2002-2012, this study investigated the different characteristics of heavy
700 rainfall in the diurnal time scale on the clean and polluted conditions respectively. Based on two indicators
701 that are AOD from MODIS aerosol product and retrieved CDNC from MODIS cloud product, we found three
702 features of heavy rainfall changing by aerosols that the rainfall start and peak time occur earlier and the
703 duration becomes longer. The quantitative differences exist between the two indicators, i.e., the statistic
704 differences of above features between clean and polluted conditions are 0.7, 1.0, 0.8 hours based on AOD and
705 1.4, 3.0, 2.2 hours based on CDNC. The different relationships of absorbing and scattering aerosols to the
706 diurnal shift were also distinguishable using ultraviolet AI from OMI and reanalysis AOD of two aerosol types
707 (BC and sulfate). The absorbing aerosols (BC) correspond to the earlier start time and peak time of heavy
708 rainfall, while the scattering aerosols (sulfate) correspond to the delayed start time and the longer duration. To
709 distinguish the influence of aerosols, the influence of moisture (SH at 850 hPa) on the heavy rainfall is also
710 investigated, which shows similar with the scattering aerosols (sulfate), that means the aerosol effect may not
711 be isolated from the impact of humidity. By comparing the characteristics of cloud macrophysics and
712 microphysics variables, using both AOD and CDNC we found the CF, ice COT, liquid and ice CWP, are
713 increased on the polluted condition, but the cloud top height and the ice CER are reduced. Liquid COT and
714 liquid CER are also increased in AOD analysis. Comparing the influence of CDNC (which represents CCN)
715 and moisture respectively on these cloud variables, the cloud properties show similar changes with the
716 increase of CDNC and moisture, but seem more sensitive to the CDNC (CCN).

717 According to these results, we speculate that both aerosol radiative effect and cloud effect have impacts on
718 the diurnal variation of heavy rainfall in the BTH region. The heating effect of absorbing aerosols especially
719 BC increases the instability of the lower to middle atmosphere so that generates the heavy rainfall occurrence
720 in advance. And the increased moisture supply and increased aerosols which nucleate more cloud droplets and
721 accumulate more liquid water in clouds, leading to the longer duration of heavy rainfall.

722 This study has clearly identified the relationship of the aerosol pollution and the diurnal changes of heavy
723 rainfall and concurrent clouds in the BTH region and attempted to address the causes. However, although this
724 work has attempted to exclude the impacts from the meteorological background particularly circulation and
725 moisture, the observation study still has its limitation on studying aerosol effect on rainfall and clouds, such as
726 the noise and uncertainty of different observational data, the interaction of aerosol and meteorological factors
727 and the mixing of different types of aerosols. Numerical model simulations are necessarily applied to examine
728 the speculation we proposed here. And the specific processes of aerosol effect on the precipitation formation
729 of mix-phased clouds also needs further exploration in our future study.

730

思媛 周 19/7/21 12:02 AM
已删除: 7

思媛 周 19/7/21 12:02 AM
已删除: roles

思媛 周 19/7/21 12:02 AM
已删除: aerosols

思媛 周 19/7/21 12:02 AM
已删除: in modifying

思媛 周 19/7/21 12:02 AM
已删除: .)

思媛 周 19/7/21 12:02 AM
已删除: (

思媛 周 19/7/21 12:02 AM
已删除: .)

思媛 周 19/7/21 12:02 AM
已删除: (liquid and ice)

思媛 周 19/7/21 12:02 AM
已删除: CCN

思媛 周 19/7/21 12:02 AM
已删除: .

思媛 周 19/7/21 12:02 AM
已删除: lead

思媛 周 19/7/21 12:02 AM
已删除: effect on

思媛 周 19/7/21 12:02 AM
已删除: cloud

思媛 周 19/7/21 12:02 AM
已删除: aerosols

思媛 周 19/7/21 12:02 AM
已删除: mix-phased cloud

746 **Data availability**

747 We are grateful to the National Meteorological Information Centre (NMIC) of the China Meteorological
748 Administration (CMA) for providing hourly precipitation datasets. MODIS aerosol and cloud data were
749 obtained from <http://ladsweb.modaps.eosdis.nasa.gov>; ultraviolet AI data from OMI was obtained from
750 <https://daac.gsfc.nasa.gov/datasets?keywords=OMI&page=1>; MACC-II and ERA-interim reanalysis datasets
751 were obtained from <http://apps.ecmwf.int/datasets>.

752 **Author contributions**

753 JY and SZ conceived the study. SZ processed data and drew the figures. SZ and JY analyzed the observational
754 results and WCW, CZ and DG gave the professional guidance. PS provided the hourly precipitation dataset.
755 SZ and JY prepared the manuscript with contributions from WCW and CZ.

756 **Competing interests**

757 The authors declare that they have no conflict of interest.

758 **Acknowledgements**

759 [Jing Yang, Daoyi Gong & Peijun Shi](#) are supported by funds from [the National Natural Science Foundation of](#)
760 [China \(41621061 and 41775071\)](#) and the National Key Research and Development Program-Global Change
761 and Mitigation Project: Global Change Risk of Population and Economic System: Mechanism and Assessment
762 (2016YFA0602401), [Siyuan Zhou](#) is supported by funds from State Key Laboratory of Earth Surface
763 Processes and Resource Ecology and Key Laboratory of Environmental Change and Natural Disaster.
764 Wei-Chyung Wang acknowledges the support of a grant (to SUNYA) from the Office of Sciences (BER), U.S.
765 DOE. [We deeply appreciate two anonymous referees for their indepth comments and constructive](#)
766 [suggestions.](#)

767

768 **References:**

769 [Ackerman, A. S.: Reduction of Tropical Cloudiness by Soot, Science, 288\(5468\), 10421047,](#)
770 [doi:10.1126/science.288.5468.1042, 2000.](#)
771 Albrecht, B. A.: Aerosols, cloud microphysics, and fractional cloudiness, *Science*, 245(4923), 1227-1230,
772 [doi:10.1126/science.245.4923.1227](#), 1989.
773 Altaratz, O., Bar-Or, R. Z., Wollner, U., and Koren, I.: Relative humidity and its effect on aerosol optical
774 depth in the vicinity of convective clouds, *Environ. Res. Lett.*, 8, 034025,
775 [doi:10.1088/1748-9326/8/3/034025](#), 2013.
776 Anonymous: [Atmospheric Sciences Thesaurus](#), China Meteorological Press: Beijing, China, 1994. (in
777 Chinese)
778 Anonymous: [IPCC fifth assessment report](#), *Weather*, 68, 310-310, 2013.

思媛 周 19/7/21 12:02 AM
已删除: This study is

思媛 周 19/7/21 12:02 AM
已删除: the National Natural Science
Foundation of China (grant nos. 41375003,
41621061 and 41575143) and Project
supported by

思媛 周 19/7/21 12:02 AM
已删除: :

思媛 周 19/7/21 12:02 AM
已删除: 1994.

思媛 周 19/7/21 12:02 AM
已删除: .

思媛 周 19/7/21 12:02 AM
已删除: (2013),

788 Bellouin, N., Quaas, J., Morcrette J. -J., and Boucher, O.: Estimates of aerosol radiative forcing from the
789 | MACC re-analysis. *Atmos. Chem. Phys.*, 13, 2045-2062, doi:10.5194/acp-13-2045-2013, 2013.

790 Benedetti, A., Morcrette, J. J., Boucher, O., Dethof, A., Engelen, R. J., Fisher, M., Flentje, H., Huneeus, N.,
791 | Jones, L., Kaiser, J. W., Kinne, S., Mangold, A., Razinger, M., Simmons, A. J., and Suttie, M.: Aerosol
792 | analysis and forecast in the European Centre for Medium-Range Weather Forecasts Integrated Forecast
793 | System: 2. Data assimilation. *J. Geophys. Res.*, 114, D13205 doi:10.1029/2008JD011115, 2009.

794 Brennan, J., Kaufman, Y., Koren, I., and Rong, L.: Aerosol-cloud interaction-Misclassification of MODIS
795 | clouds in heavy aerosol, *IEEE T. Geosci. Remote.*, 43, 911-915, doi:10.1109/TGRS.2005.844662, 2005.

796 Bennartz, R., and Rausch, J.: Global and regional estimates of warm cloud droplet number concentration
797 | based on 13 years of AQUA-MODIS observations, *Atmos. Chem. Phys.*, 17, 9815-9836,
798 | doi:10.5194/acp-17-9815-2017, 2017.

799 Bennartz, R.: Global assessment of marine boundary layer cloud droplet number concentration from satellite, *J.*
800 | *Geophys. Res.*, 112, D02201, doi:10.1029/2006JD007547, 2007.

801 Boers, R., Acarreta, J. A., and Gras, J. L.: Satellite monitoring of the first indirect aerosol effect: Retrieval of
802 | the droplet concentration of water clouds, *J. Geophys. Res.*, 111, D22208, doi:10.1029/2005JD006838,
803 | 2006.

804 | [Boucher, O., and Quaas, J.: Water vapour affects both rain and aerosol optical depth, *Nat. Geosci.*, 6\(1\), 45,
805 | doi:10.1038/ngeo1692, 2012.](#)

806 Chen, Q., Yin, Y., Jin, L., Xiao, H., and Zhu, S.: The effect of aerosol layers on convective cloud
807 | microphysics and precipitation, *Atmos. Res.*, 101, 327-340, doi:10.1016/j.atmosres.2011.03.007, 2011.

808 Cheng, C. T., Wang, W. C., and Chen, J. P.: A modeling study of aerosol impacts on cloud microphysics and
809 | radiative properties, *Q. J. R. Meteorol. Soc.*, 133, 283-297, doi:10.1002/qj.25, 2007.

810 Cheng, C. T., Wang, W. C., and Chen, J. P.: Simulation of the effects of increasing cloud condensation nuclei
811 | on mixed-phase clouds and precipitation of a front system. *Atmos. Res.*, 96, 461-476, doi:
812 | 10.1016/j.atmosres.2010.02.005, 2010.

813 Chylek, P., Dubey, M. K., Lohmann, U., Ramanathan, V., Kaufman, Y. J., Lesins, G., Hudson, J., Altmann,
814 | G., and Olsen, S.: Aerosol indirect effect over the Indian Ocean, *Geophys. Res. Lett.*, 33(6), L06806,
815 | doi:10.1029/2005GL025397, 2006.

816 Dee, D. P., Uppala, S. M., Simmons, A. J., Berrisford, P., Poli, P., Kobayashi, S., Andrae, U., Balmaseda, M.
817 | A., Balsamo, G., Bauer, P., Bechtold, P., Beljaars, A. C. M., van de Berg, L., Bidlot, J., Bormann, N.,
818 | Delsol, C., Dragani, R., Fuentes, M., Geer, A. J., Haimberger, L., Healy, S. B., Hersbach, H., H'olm, E.
819 | V., Isaksen, I., K'allberg, P., K'ohler, M., Matricardi, M., McNally, A. P., Monge-Sanz, B. M.,
820 | Morcrette, J. -J., Park, B. -K., Peubey, C., de Rosnay, P., Tavolato, C., Th'epaut, J. -N., Vitart, F.: The
821 | ERA-Interim reanalysis: configuration and performance of the data assimilation system. *Q. J. R.*
822 | *Meteorol. Soc.*, 137, 553-597, doi:10.1002/qj.828, 2011.

823 Fan, J. W., Rosenfeld, D., Yang, Y., Zhao, C., Leung, L. R., and Li, Z. Q.: Substantial contribution of

思媛 周 19/7/21 12:02 AM
已删除:.
思媛 周 19/7/21 12:02 AM
已删除:.

思媛 周 19/7/21 12:02 AM
已删除:.
思媛 周 19/7/21 12:02 AM
已删除:.
思媛 周 19/7/21 12:02 AM
已删除:.
思媛 周 19/7/21 12:02 AM
已删除: https://
思媛 周 19/7/21 12:02 AM
已删除: .org/
思媛 周 19/7/21 12:02 AM
已删除:.

思媛 周 19/7/21 12:02 AM
已设置格式: 字体:非 加粗
思媛 周 19/7/21 12:02 AM
已删除: 2011.

思媛 周 19/7/21 12:02 AM
已删除:.
思媛 周 19/7/21 12:02 AM
已删除:.

思媛 周 19/7/21 12:02 AM
已删除:.
思媛 周 19/7/21 12:02 AM
已删除:.
思媛 周 19/7/21 12:02 AM
已删除:.
思媛 周 19/7/21 12:02 AM
已删除:.

839 anthropogenic air pollution to catastrophic floods in Southwest China. *Geophys. Res. Lett.*, 42,
840 6066-6075, doi:10.1002/2015GL064479, 2015.

841 Garrett, T. J. and Zhao, C.: Increased Arctic cloud longwave emissivity associated with pollution from
842 mid-latitudes. *Nature*, 440(7085), 787-9, doi:10.1038/nature04636, 2006.

843 Givati, A., and Rosenfeld, D.: Quantifying precipitation suppression due to air pollution. *J. Appl. Meteor.*, 43,
844 1038-1056, doi:10.1175/1520-0450(2004)043<1038:QPSDTA>2.0.CO;2, 2004.

845 Grandey, B. S., and Stier, P.: A critical look at spatial scale choices in satellite-based aerosol indirect effect
846 studies. *Atmos. Chem. Phys.*, 10(23), 11459–11470, doi:10.5194/acp-10-11459-2010, 2010.

847 Grandey, B. S., Stier, P. and Wagner, T. M.: Investigating relationships between aerosol optical depth and
848 cloud fraction using satellite, aerosol reanalysis and general circulation model data. *Atmos. Chem. Phys.*,
849 13(6), 31773184, doi:10.5194/acp-13-3177-2013, 2013.

850 Gryspeerdt, E., Sourdeval, O., Quaas, J., Delanoë, J., Krämer, M., and Kühne, P.: Ice crystal number
851 concentration estimates from lidar–radar satellite remote sensing – Part 2: Controls on the ice crystal
852 number concentration, *Atmos. Chem. Phys.*, 18(19), 14351–14370, doi:10.5194/acp-18-14351-2018,
853 2018.

854 Gryspeerdt, E., Stier, P., and Grandey, B. S.: Cloud fraction mediates the aerosol optical depth-cloud top
855 height relationship. *Geophys. Res. Lett.*, 41, 36223627, doi:10.1002/2014GL059524, 2014a.

856 Gryspeerdt, E., Stier, P., and Partridge, D. G.: Links between satellite-retrieved aerosol and precipitation.
857 *Atmos. Chem. Phys.*, 14, 9677–9694, doi:10.5194/acp-14-9677-2014, 2014b.

858 Gunthe, S. S., Rose, D., Su, H., Garland, R. M., Achtert, P., Nowak, A., Wiedensohler, A., Kuwata, M.,
859 Takegawa, N., Kondo, Y., Hu, M., Shao, M., Zhu, T., Andreae, M. O., and Poschl, U.: Cloud
860 condensation nuclei (CCN) from fresh and aged air pollution in the megacity region of Beijing, *Atmos.*
861 *Chem. Phys.*, 11(21), 11023-11039, doi:10.5194/acp-11-11023-2011, 2011.

862 Guo, C. W., Xiao, H., Yang, H. L., and Tang, Q.: Observation and modeling analyses of the macro-and
863 microphysical characteristics of a heavy rain storm in Beijing, *Atmos. Res.*, 156, 125-141,
864 doi:10.1016/j.atmosres.2015.01.007, 2015.

865 Guo, J. P., Deng, M. J., Lee, S. S., Wang, F., Li, Z. Q., Zhai, P. M., Liu, H., Lv, W., Yao, W., and Li, X. W.:
866 Delaying precipitation and lightning by air pollution over the Pearl River Delta. Part I: Observational
867 analyses. *J. Geophys. Res. Atmos.*, 121, 6472-6488, doi:10.1002/2015JD023257, 2016.

868 Guo, L., Highwood, E. J., Shaffrey, L. C., and Turner, A. G.: The effect of regional changes in anthropogenic
869 aerosols on rainfall of the East Asian Summer Monsoon. *Atmos. Chem. Phys.*, 13, 1521-1534,
870 doi:10.5194/acp-13-1521-2013, 2013.

871 Guo, X. L., Fu, D. H., Guo, X., and Zhang, C. M.: A case study of aerosol impacts on summer convective
872 clouds and precipitation over northern China. *Atmos. Res.*, 142, 142-157,
873 doi:10.1016/j.atmosres.2013.10.006, 2014.

874 Hammer, M. S., Martin, R. V., Li, C., Torres, O., Manning, M., and Boys, B. L.: Insight into global trends in

思媛周 19/7/21 12:02 AM

已删除:

思媛周 19/7/21 12:02 AM

已删除:

思媛周 19/7/21 12:02 AM

已删除:

思媛周 19/7/21 12:02 AM

已删除:

思媛周 19/7/21 12:02 AM

已删除:

思媛周 19/7/21 12:02 AM

已删除:

思媛周 19/7/21 12:02 AM

已删除:

思媛周 19/7/21 12:02 AM

已删除:

思媛周 19/7/21 12:02 AM

已删除:

思媛周 19/7/21 12:02 AM

已删除:

思媛周 19/7/21 12:02 AM

已删除:

思媛周 19/7/21 12:02 AM

已删除:

思媛周 19/7/21 12:02 AM

已删除:

思媛周 19/7/21 12:02 AM

已删除:

思媛周 19/7/21 12:02 AM

已删除:

思媛周 19/7/21 12:02 AM

已删除:

思媛周 19/7/21 12:02 AM

已删除:

思媛周 19/7/21 12:02 AM

已删除:

思媛周 19/7/21 12:02 AM

已删除:

思媛周 19/7/21 12:02 AM

已删除:

思媛周 19/7/21 12:02 AM

已删除:

思媛周 19/7/21 12:02 AM

已删除:

思媛周 19/7/21 12:02 AM

已删除:

思媛周 19/7/21 12:02 AM

已删除:

思媛周 19/7/21 12:02 AM

已删除:

898 aerosol composition from 2005 to 2015 inferred from the OMI Ultraviolet Aerosol Index, *Atmos. Chem.*
899 *Phys.*, 18, 8097-8112, doi:10.5194/acp-18-8097-2018, 2018.

900 Harikishan, G., Padmakumari, B., Maheskumar, R. S., Pandithurai, G., and Min, Q. L.: Aerosol indirect effects
901 from ground-based retrievals over the rain shadow region in Indian subcontinent, *J. Geophys. Res.*
902 *Atmos.*, 121(5), 2369-2382, doi:10.1002/2015JD024577, 2016.

903 Higgins, R. W., Yao, Y., Yarosh, E. S., Janowiak, J. E. and Mo, K. C.: Influence of the Great Plains low-level
904 jet on summertime precipitation and moisture transport over the central United States, *J. Climate*, 10,
905 481-507, doi:10.1175/1520-0442(1997)010<0481:IOTGPI>2.0.CO;2, 1997.

906 Holz, R. E., Ackerman, S. A., Nagle, F. W., Frey, R., Dutcher, S., Kuehn, R. E., Vaughan, M. A., and Baum,
907 B.: Global Moderate Resolution Imaging Spectroradiometer (MODIS) cloud detection and height
908 evaluation using CALIOP, *J. Geophys. Res. Atmos.*, 113, D00A19, doi: 10.1029/2008JD009837, 2008.

909 Jacobson, M. Z.: Strong radiative heating due to the mixing state of black carbon in atmospheric aerosols,
910 *Nature*, 409, 695-697, doi:10.1038/35055518, 2001.

911 Jiang, H., Feingold, G., and Cotton, W. R.: Simulations of aerosol-cloud-dynamical feedbacks resulting from
912 entrainment of aerosol into the marine boundary layer during the Atlantic Stratocumulus Transition
913 Experiment, *J. Geophys. Res.*, 107(D24), 4813, doi:10.1029/2001JD001502, 2002.

914 Jiang, J. H., Su, H., Schoeberl, M. R., Massie, S. T., Colarco, P., Platnick, S., and Livesey, N. J.: Clean and
915 polluted clouds: Relationships among pollution, ice clouds, and precipitation in South America, *Geophys.*
916 *Res. Lett.*, 35, L14804, doi: 10.1029/2008GL034631, 2008.

917 Jiang, M. J., Li, Z. Q., Wan, B. C., and Cribb, M.: Impact of aerosols on precipitation from deep convective
918 clouds in eastern China, *J. Geophys. Res.*, 121, 9607-9620, doi:10.1002/2015JD024246, 2016.

919 Johnson, D. B.: The role of giant and ultra-giant aerosol particles in warm rain initiation, *J. Atmos. Sci.*, 39,
920 448-460, doi:10.1175/1520-0469(1982)039<0448:TROGAU>2.0.CO;2, 1982.

921 Jung, W. S., Panicker, A. S., Lee, D. I., and Park, S. H.: Estimates of aerosol indirect effect from Terra
922 MODIS over Republic of Korea, *Advances in Meteorology*, 2013 (976813), 1-8,
923 doi:10.1155/2013/976813, 2013.

924 Kim, K.-M., Lau, K. M., Sud, Y. C., and Walker, G. K.: Influence of aerosol radiative forcings on the diurnal
925 and seasonal cycles of rainfall over West Africa and Eastern Atlantic Ocean using GCM simulation, *Clim.*
926 *Dyn.*, 35(1), 115-126, doi: 10.1007/s00382-010-0750-1, 2010.

927 Lau, K. M., Kim, M. K., and Kim, K. M.: Asian summer monsoon anomalies induced by aerosol direct
928 forcing: the role of the Tibetan Plateau, *Clim. Dyn.*, 26, 855-864, doi:10.1007/s00382-006-0114-z, 2006.

929 Lee, S. S., Donner, L. J., and Phillips, V. T. J.: Impacts of aerosol chemical composition on microphysics and
930 precipitation in deep convection, *Atmos. Res.*, 94, 220-237, doi:10.1016/j.atmosres.2009.05.015, 2009.

931 Lee, S. S., Guo, J., and Li, Z.: Delaying precipitation by air pollution over the Pearl River Delta: 2. Model
932 simulation, *J. Geophys. Res. Atmos.*, 121, 11739-11760, doi:10.1002/2015JD024362, 2016.

933 Lelieveld, J. and Heintzenberg, J.: Sulfate cooling effect on climate through in-cloud oxidation of

思媛周 19/7/21 12:02 AM

已删除:

思媛周 19/7/21 12:02 AM

已删除:

思媛周 19/7/21 12:02 AM

已删除:)

思媛周 19/7/21 12:02 AM

已设置格式: 定义网格后不调整右缩进, 行距: 1.5 倍行距, 不对齐到网格

思媛周 19/7/21 12:02 AM

已删除:

思媛周 19/7/21 12:02 AM

已删除:

思媛周 19/7/21 12:02 AM

已删除:

思媛周 19/7/21 12:02 AM

已删除:

思媛周 19/7/21 12:02 AM

已删除:

思媛周 19/7/21 12:02 AM

已删除:

思媛周 19/7/21 12:02 AM

已删除:)

思媛周 19/7/21 12:02 AM

已删除: http://dx.

思媛周 19/7/21 12:02 AM

已删除: .org/

思媛周 19/7/21 12:02 AM

已删除:

思媛周 19/7/21 12:02 AM

已删除:

思媛周 19/7/21 12:02 AM

已删除:)

思媛周 19/7/21 12:02 AM

已删除:

思媛周 19/7/21 12:02 AM

已删除:

思媛周 19/7/21 12:02 AM

已删除:

思媛周 19/7/21 12:02 AM

已删除:

思媛周 19/7/21 12:02 AM

已删除:

954 anthropogenic SO₂, *Science*, 258, 117-120, doi:10.1126/science.258.5079.117, 1992.

955 Levy, R. C., Mattoo, S., Munchak, L. A., Remer, L. A., Sayer, A. M., Patadia, F., and Hsu, N. C.: The
956 Collection 6 MODIS aerosol products over land and ocean, *Atmos. Meas. Tech.*, 6, 2989–3034,
957 doi:10.5194/amt-6-2989-2013, 2013.

958 Li, H., Cui, X., Zhang, W., and Qiao, L.: Observational and dynamic downscaling analysis of a heavy rainfall
959 event in Beijing, China during the 2008 Olympic Games, *Atmos. Sci. Lett.*, 17, 368-376,
960 doi:10.1002/asl.667, 2016.

961 Li, Z., Niu, F., Fan, J., Liu, Y., Rosenfeld, D., and Ding, Y.: Long-term impacts of aerosols on the vertical
962 development of clouds and precipitation, *Nat. Geosci.*, 4, 888-894, doi:10.1038/ngeo1313, 2011.

963 Lim, K. S. and Hong, S.: Investigation of aerosol indirect effects on simulated flash-flood heavy rainfall over
964 Korea, *Meteor. Atmos. Phys.*, 118, 199-214, doi:10.1007/s00703-012-0216-6, 2012.

965 Liu, G., Shao, H., Coakley Jr. J. A., Curry, J. A., Haggerty, J. A., and Tschudi, M. A.: Retrieval of cloud
966 droplet size from visible and microwave radiometric measurements during INDOEX: Implication to
967 aerosols' indirect radioactive effect, *J. Geophys. Res.*, 108(D1), 4006, doi:10.1029/2001JD001395, 2003.

968 Liu, J., Wang, S., Zhang, W., and Wei, X.: Mechanism analysis of a strong convective weather in Hebei
969 Province, *Advances in Marine Science*, 30, 9-16, 2012. (in Chinese)

970 Menzel, W. P., Frey, R. A., Zhang, H., Wylie, D. P., Moeller, C. C., Holz, R. E., Maddux, B., Baum, B. A.,
971 Strabala, K. I., and Gumley, L. E.: MODIS global cloud-top pressure and amount estimation: Algorithm
972 description and results, *J. Appl. Meteorol. Clim.*, 47(4), 1175-1198, doi: 10.1175/2007JAMC1705.1,
973 2008.

974 Min, Q., Joseph, E., Lin, Y., Min, L., Yin, B., Daum, P. H., Kleinman, L. I., Wang, J., and Lee, Y. -N.:
975 Comparison of MODIS cloud microphysical properties with in-situ measurements over the Southeast
976 Pacific, *Atmos. Chem. Phys.*, 12, 11261-11273, doi:10.5194/acp-12-11261-2012, 2012.

977 Nakajima, T. and King, M. D.: Determination of the optical thickness and effective particle radius of clouds
978 from reflected solar radiation measurements. Part I: Theory, *J. Atmos. Sci.*, 47, 1878-1893,
979 doi:10.1175/1520-0469(1990)047<1878:DOTOTA>2.0.CO;2, 1990.

980 Panicker, A. S., Pandithurai, G., and Dipu, S.: Aerosol indirect effect during successive contrasting monsoon
981 seasons over Indian subcontinent using MODIS data, *Atmos. Environ.*, 44(15), 1937-1943,
982 doi:10.1016/j.atmosenv.2010.02.015, 2010.

983 Platnick, S., Meyer, K., King, M. D., Wind, G., Amarasinghe, N., Marchant, B., Arnold, G. T., Zhang, Z.,
984 Hubanks, P. A., Holz, R. E., Yang, P., Ridgway, W. L., and Riedi, J.: The MODIS cloud optical and
985 microphysical products: Collection 6 updates and examples from Terra and Aqua, *IEEE Trans. Geosci.*
986 *Remote Sens.*, 55, 502-525, doi:10.1109/TGRS.2016.2610522, 2017.

987 Qian, Y., Gong, D. Y., Fan, J. W., Leung, L. R., Bennartz, R., Chen, D. L., Wang, W. G.: Heavy pollution
988 suppresses light rain in China: Observations and modeling, *J. Geophys. Res. Atmos.*, 114, D00K02,
989 doi:10.1029/2008JD011575, 2009.

思媛 周 19/7/21 12:02 AM

已删除:

思媛 周 19/7/21 12:02 AM

已删除:

思媛 周 19/7/21 12:02 AM

已删除: https://

思媛 周 19/7/21 12:02 AM

已删除: .org/

思媛 周 19/7/21 12:02 AM

已设置格式: 字体:非 加粗

思媛 周 19/7/21 12:02 AM

已删除:)

思媛 周 19/7/21 12:02 AM

已删除:

思媛 周 19/7/21 12:02 AM

已删除: Atmospheric environment

思媛 周 19/7/21 12:02 AM

已删除:)

思媛 周 19/7/21 12:02 AM

已删除:

思媛 周 19/7/21 12:02 AM

已删除:

思媛 周 19/7/21 12:02 AM

已删除:

思媛 周 19/7/21 12:02 AM

已设置格式: 字体:非 加粗

思媛 周 19/7/21 12:02 AM

已删除:

思媛 周 19/7/21 12:02 AM

已设置格式: 字体:非 加粗

.002 Qiu, Y., Zhao, C., Guo, J., and Li, J.: 8-Year ground-based observational analysis about the seasonal variation
.003 of the aerosol-cloud droplet effective radius relationship at SGP site, *Atmos. Environ.*, 164, 139-146,
.004 [doi:10.1016/j.atmosenv.2017.06.002](https://doi.org/10.1016/j.atmosenv.2017.06.002), 2017.

.005 Quaas, J., Boucher, O., Bellouin, N. and Kinne, S.: Satellite-based estimate of the direct and indirect aerosol
.006 climate forcing, *J. Geophys. Res.*, 113, D05204, doi:10.1029/2007JD008962, 2008.

.007 [Quaas, J., Stevens, B., Stier, P., and Lohmann U.: Interpreting the cloud cover aerosol optical depth
.008 relationship found in satellite data using a general circulation model, *Atmos. Chem. Phys.*, 10\(13\),
.009 6129-6135, doi:10.5194/acp-10-6129-2010, 2010.](https://doi.org/10.5194/acp-10-6129-2010)

.010 Rienecker, M. M., Suarez, M. J., Todling, R., Bacmeister, J., Takacs, L., Liu, H. C., Gu, W., Sienkiewicz, M.,
.011 Koster, R. D., Gelaro, R., Stajner, I., Nielsen, J. E.: The GEOS-5 Data Assimilation
.012 System—Documentation of Versions 5.0.1 and 5.1.0, and 5.2.0. NASA Technical Report Series on
.013 Global Modeling and Data Assimilation NASA/TM-2008-104606 27: 92 pp, 2008.

.014 Rosenfeld, D.: TRMM observed first direct evidence of smoke from forest fires inhibiting rainfall, *Geophys.*
.015 *Res. Lett.*, 26, 3105–3108, doi:10.1029/1999GL006066, 1999.

.016 Rosenfeld, D., Lohmann, U., Raga, G. B., O'Dowd, C. D., Kulmala, M., Fuzzi, S., Reissell, A., Andreae, M.
.017 O.: Flood or drought: How do aerosols affect precipitation? *Science*, 321, 1309-1313,
.018 [doi:10.1126/science.1160606](https://doi.org/10.1126/science.1160606), 2008.

.019 Rosenfeld, D., Sherwood, S., Wood, R., and Donner, L.: Climate effects of aerosol-cloud interactions, *Science*,
.020 343, 379-380, doi:10.1126/science.1247490, 2014.

.021 Rosenfeld, D., and Woodley, W. L.: Convective clouds with sustained highly supercooled liquid water down
.022 to -37.5°C , *Nature*, 405, 440–442, doi:10.1038/35013030, 2000.

.023 Sassen, K., Starr, D., Mace, G. G., Poellot, M. R., Melfi, S. H., Eberhard, W.L., Spinhirne, J. D., Eloranta, E.
.024 W., Hagan, D. E., and Hallett, J.: The 5–6 December 1991 FIRE IFO II jet stream cirrus case study:
.025 Possible influences of volcanic aerosols, *J. Atmos. Sci.*, 52, 97–123, doi:10.1175/1520-0469(1995)
.026 052<0097:TDFIJJ>2.0.CO;2, 1995.

.027 Shen, Y., Xiong, A., Wang, Y., and Xie, P.: Performance of high-resolution satellite precipitation products
.028 over China, *J. Geophys. Res.*, 115, D02114, doi:10.1029/2009JD012097, 2010.

.029 Sherwood, S.: Aerosols and ice particle size in tropical cumulonimbus, *J. Clim.*, 15, 1051–1063,
.030 doi:10.1175/1520-0442(2002)015<1051:AAIPSI>2.0.CO;2, 2002.

.031 Shinozuka, Y., Clarke, A. D., Nenes, A., Jefferson, A., Wood, R., McNaughton, C. S., Ström, J., Tunved, P.,
.032 Redemann, J., Thornhill, K. L., Moore, R. H., Latham, T. L., Lin, J. J., and Yoon, Y. J.: The relationship
.033 between cloud condensation nuclei (CCN) concentration and light extinction of dried particles:
.034 indications of underlying aerosol processes and implications for satellite-based CCN estimates, *Atmos.*
.035 *Chem. Phys.*, 15, 7585-7604, doi:10.5194/acp-15-7585-2015, 2015.

.036 Song, X. L. and Zhang, G. J.: Microphysics parameterization for connective clouds in a global climate model:
.037 Description and single-column model tests, *J. Geophys. Res. Atmos.*, 116, D02201,

思媛周 19/7/21 12:02 AM

已删除:

思媛周 19/7/21 12:02 AM

已删除:

思媛周 19/7/21 12:02 AM

已删除:

思媛周 19/7/21 12:02 AM

已删除:

思媛周 19/7/21 12:02 AM

已删除:

思媛周 19/7/21 12:02 AM

已删除:

思媛周 19/7/21 12:02 AM

已删除:

思媛周 19/7/21 12:02 AM

已删除:

.046 | [doi:10.1029/2010JD014833](https://doi.org/10.1029/2010JD014833), 2011.

.047 | Squires, P.: The growth of cloud drops by condensation: I. general characteristics, *Aust. J. Sci. Res., Ser. A*, 5,
.048 | 66–86, 1952.

.049 | Squires, P., and Twomey, S.: A comparison of cloud nucleus measurements over central North America and
.050 | Caribbean Sea, *J. Atmos. Sci.*, 23, 401–404, doi: 10.1175/1520-0469(1966)023<0401:ACOCNM>
.051 | -2.0.CO;2, 1966.

.052 | Sun, Y. L., Wang, Z. F., Du, W., Zhang, Q., Wang, Q. Q., Fu, P. Q., Pan, X. L., Li, J., Jayne, J., and Worsnop,
.053 | D. R.: Long-term real-time measurements of aerosol particle composition in Beijing, China: seasonal
.054 | variations, meteorological effects, and source analysis, *Atmos. Chem. Phys.*, 15, 10149–10165,
.055 | [doi:10.5194/acp-15-10149-2015](https://doi.org/10.5194/acp-15-10149-2015), 2015.

.056 | Tariq, S., and Ali, M.: Spatio-temporal distribution of absorbing aerosols over Pakistan retrieved from OMI on
.057 | board Aura Satellite, *Atmos. Pollution Res.*, doi: 10.5094/APR.2015.030, 2015.

.058 | Tao, M. H., Chen, L. F., Wang, Z. F., Tao, J. H., Che, H. Z., Wang, X. H., and Wang, Y.: Comparison and
.059 | evaluation of the MODIS Collection 6 aerosol data in China, *J. Geophys. Res. Atmos.*, 120, 6992–7005,
.060 | [doi:10.1002/2015JD023360](https://doi.org/10.1002/2015JD023360), 2015.

.061 | Tao, W. K., Chen, J. P., Li, Z., Wang, C., and Zhang C.: Impact of aerosols on convective clouds and
.062 | precipitation, *Rev. Geophys.*, 50, RG2001/2012, 1–62, doi: 10.1029/2011RG000369, 2012.

.063 | Torres, O., Bhartia, P.K., Herman, J.R., Ahmad, Z., Gleason, J.: Derivation of aerosol properties from satellite
.064 | measurements of backscattered ultraviolet radiation: Theoretical basis, *J. Geophys. Res. Atmos.*, 103,
.065 | 17099–17110, [doi:10.1029/98JD00900](https://doi.org/10.1029/98JD00900), 1998.

.066 | Twohy, C. H., Coakley, J. A., and Tahnk, W. R.: Effect of changes in relative humidity on aerosol scattering
.067 | near clouds, *J. Geophys. Res. Atmos.*, 114, D05205, [doi:10.1029/2008JD010991](https://doi.org/10.1029/2008JD010991), 2009.

.068 | Twomey, S.: The influence of pollution on the shortwave albedo of clouds, *J. Atmos. Sci.*, 34, 1149–1152,
.069 | doi:10.1175/1520-0469(1977)034<1149:TIOPOT>2.0.CO;2, 1977.

.070 | Wang, J., Feng, J., Wu, Q., and Z. Yan, Z.: Impact of anthropogenic aerosols on summer precipitation in the
.071 | Beijing-Tianjin-Hebei urban agglomeration in China: Regional climate modeling using WRF-Chem, *Adv.*
.072 | *Atmos. Sci.*, 33, 753–766, [doi:10.1007/s00376-015-5103-x](https://doi.org/10.1007/s00376-015-5103-x), 2016.

.073 | Wolyn, P. G., and Mckee, T. B.: The mountain plains circulation east of a 2-km-high north south barrier, *Mon.*
.074 | *Weather Rev.*, 122, 1490–1508, [doi:10.1175/1520-0493\(1994\)122<1490:TMPCEO>2.0.CO;2](https://doi.org/10.1175/1520-0493(1994)122<1490:TMPCEO>2.0.CO;2), 1994.

.075 | Wu, P., Ding, Y. H., and Liu, Y. J.: Atmospheric circulation and dynamic mechanism for persistent haze
.076 | events in the Beijing-Tianjin-Hebei region, *Adv. Atmos. Sci.*, 34(4), 429–440,
.077 | [doi:10.1007/s00376-016-6158-z](https://doi.org/10.1007/s00376-016-6158-z), 2017.

.078 | Yang, X., Zhao, C., Zhou, L., Li, Z., Cribb, M., and Yang, S.: Wintertime cooling and a potential connection
.079 | with transported aerosols in Hong Kong during recent decades, *Atmos. Res.*, 211, 52–61,
.080 | [doi:10.1016/j.atmosres.2018.04.029](https://doi.org/10.1016/j.atmosres.2018.04.029), 2018.

.081 | Yu, R. C., Zhou, T. J., Xiong, A. Y., Zhu, Y. J., and Li, J. M.: Diurnal variations of summer precipitation over

思媛周 19/7/21 12:02 AM
已删除:

思媛周 19/7/21 12:02 AM
已删除:

思媛周 19/7/21 12:02 AM
已删除:

思媛周 19/7/21 12:02 AM
已删除:

思媛周 19/7/21 12:02 AM
已删除:

思媛周 19/7/21 12:02 AM
已删除:

思媛周 19/7/21 12:02 AM
已删除:

思媛周 19/7/21 12:02 AM
已删除:

思媛周 19/7/21 12:02 AM
已删除:

思媛周 19/7/21 12:02 AM
已删除:

思媛周 19/7/21 12:02 AM
已删除: Journal of Geophysical Research: Atmospheres, 114, n/a-n/a,

思媛周 19/7/21 12:02 AM
已删除:

思媛周 19/7/21 12:02 AM
已设置格式: 字体:非 加粗

思媛周 19/7/21 12:02 AM
已删除: Wang, Z., Guo, P., and Zhang, H.: A Numerical Study of Direct Radiative Forcing Due to Black Carbon and Its Effects on the Summer Precipitation in China. *Climatic and Environmental Research*, 14, 161–171, 2009.

思媛周 19/7/21 12:02 AM
已设置格式: 定义网格后不调整右缩进, 行距: 1.5 倍行距, 不对齐到网格

思媛周 19/7/21 12:02 AM
已删除:)

思媛周 19/7/21 12:02 AM
已删除:

思媛周 19/7/21 12:02 AM
已删除:

思媛周 19/7/21 12:02 AM
已删除:

.106 | contiguous China. *Geophys. Res. Lett.* 34, L017041. doi:10.1029/2006GL028129, 2007.

.107 | Yuan, T., Li, Z., Zhang, R., and Fan, J.: Increase of cloud droplet size with aerosol optical depth: An
.108 | observation and modeling study. *J. Geophys. Res. Atmos.*, 113, D04201. doi:10.1029/2007JD008632,
.109 | 2008.

.110 | Yuan, W. H., Yu, R. C., Chen, H. M., Li, J., and Zhang, M. H.: Subseasonal Characteristics of Diurnal
.111 | Variation in Summer Monsoon Rainfall over Central Eastern China. *J. Climate*, 23, 6684-6695.
.112 | doi:10.1175/2010JCLI3805.1, 2010.

.113 | Zeng, S., Riedi, J., Trepte, C. R., Winker, D. M., and Hu, Y. -X.: Study of global cloud droplet number
.114 | concentration with A-Train satellites. *Atmos. Chem. Phys.*, 14, 7125-7134, doi:
.115 | 10.5194/acp-14-7125-2014, 2014.

.116 | Zhao, B., Gu, Y., Liou, K. -N., Wang, Y., Liu, X., Huang, L., Jiang, J. H., and Su, H.: Type-Dependent
.117 | Responses of Ice Cloud Properties to Aerosols From Satellite Retrievals, *Geophys. Res. Lett.*, 45(7),
.118 | 3297-3306, doi:10.1002/2018GL077261, 2018.

.119 | Zhou, S., Yang, J., Wang, W. C., Gong, D., Shi, P., and Gao, M.: Shift of daily rainfall peaks over the
.120 | Beijing-Tianjin-Hebei region: An indication of pollutant effects? *Int. J. Climatol.* 2018, 1-10.
.121 | doi:10.1002/joc.5700, 2018.

.122 | Zhu, Y., Rosenfeld, D., and Li, Z.: Under what conditions can we trust retrieved cloud drop concentrations in
.123 | broken marine stratocumulus? *J. Geophys. Res. Atmos.*, 123, 8754-8767. doi:10.1029/2017JD028083,
.124 | 2018.

思媛 周 19/7/21 12:02 AM
已删除:.

思媛 周 19/7/21 12:02 AM
已删除:.

思媛 周 19/7/21 12:02 AM
已删除:.

思媛 周 19/7/21 12:02 AM
已删除:.

思媛 周 19/7/21 12:02 AM
已删除:.

思媛 周 19/7/21 12:02 AM
已删除:.

思媛 周 19/7/21 12:02 AM
已删除:.

思媛 周 19/7/21 12:02 AM
已删除:.

思媛 周 19/7/21 12:02 AM
已删除:.

思媛 周 19/7/21 12:02 AM
已设置格式: 字体:Times, 11 pt

思媛 周 19/7/21 12:02 AM
已删除:.

思媛 周 19/7/21 12:02 AM
已删除:.

思媛 周 19/7/21 12:02 AM
已删除:.

思媛 周 19/7/21 12:02 AM
已删除: https://

思媛 周 19/7/21 12:02 AM
已删除: .org/

思媛 周 19/7/21 12:02 AM
已删除:.

思媛 周 19/7/21 12:02 AM
已删除: .

思媛 周 19/7/21 12:02 AM
已设置格式: 缩进: 左: 0 cm, 悬挂缩进: 2 字符, 首行缩进: -2 字符

.159
.160

.161
.162
.163
.164
.165
.166
.167

.168
.169
.170
.171
.172
.173
.174
.175

Tables

Indicator	Source	Begin time	Thresholds	
			25 th percentile	75 th percentile
AOD	MODIS	2002	0.98	2.00
CDNC (cm ⁻³)	MODIS	2002	30.10	91.03
AAI	OMI	2005	0.13	0.52
SAI	OMI	2005	- 0.13	- 0.35
AOD of BC	MACC	2003	0.04	0.06
AOD of sulfate	MACC	2003	0.46	0.87
SH at 850 hPa (g/kg)	ERA-interim	2002	9.96	12.95

Table 1. The indicators and their sources, begin times and the thresholds used in the study. The end time of all data is to 2012.

Characteristics of heavy rainfall	Clean		Polluted		Difference		Significance	
	AOD	CDNC	AOD	CDNC	AOD	CDNC	AOD	CDNC
Start time	24.2 (3.9)	24.3 (4.0)	23.5 (4.8)	22.9 (3.9)	- 0.7	- 1.4	P<0.05	P<0.05
Peak time	23.0 (4.0)	22.1 (5.3)	22.0 (4.8)	19.1 (5.7)	- 1.0	- 3.0	P<0.05	P<0.05
Duration	4.0 (2.1)	5.5 (3.3)	4.8 (2.8)	7.7 (4.3)	0.8	2.2	P<0.05	P<0.05
Intensity	164.9 (98.4)	166.0 (89.3)	169.6 (94.3)	162.7 (89.1)	4.7	- 3.3	P>0.1	P>0.1

Table 2. The mean values of start time (units: LST), peak time (units: LST), duration (units: hours) and intensity (units: 0.1mm/hour) of heavy rainfall respectively on the clean and polluted conditions using two indicators of AOD and CDNC, and their differences (polluted minus clean) and significances. The numbers in the brackets stand for the standard deviations on the means. "P<0.05" stands for the difference has passed the significance test of 95%, and "P>0.1" stands for the difference did not pass the significance test of 90%.

思媛周 19/7/21 12:02 AM
已删除: [2]

思媛周 19/7/21 12:02 AM
已删除: used in the study
思媛周 19/7/21 12:02 AM
已删除: for clean/less and polluted/more conditions

思媛周 19/7/21 12:02 AM
已删除: [3]

思媛周 19/7/21 12:02 AM
已删除: average

思媛周 19/7/21 12:02 AM
已删除: the
思媛周 19/7/21 12:02 AM
已删除: between clean and polluted conditions

Characteristics of heavy rainfall	AAI	SAI	Difference (AAI-SAI)	Less BC	More BC	Difference (More-Less)	Less sulfate	More sulfate	Difference (More-Less)
Start time	23.4 (4.8)	24.1 (4.4)	-0.7	24.2 (4.8)	23.9 (4.4)	-0.3	24.0 (4.3)	24.5 (4.4)	0.5
Peak time	21.0 (5.3)	22.6 (5.1)	-1.6	23.4 (5.3)	22.3 (4.0)	-1.1	23.2 (4.5)	22.9 (4.8)	-0.3
Duration	5.0 (3.1)	6.0 (3.8)	-1.0	4.8 (2.6)	4.6 (2.7)	-0.2	4.0 (2.1)	5.5 (3.0)	1.5

思媛周 19/7/21 12:02 AM

Characteristics of heavy rainfall	AAI	SAI
Start time (LST)	23.4	24.1
Peak time (LST)	21.0	22.6
Duration (hours)	5.0	6.0

已删除:

思媛周 19/7/21 12:02 AM

已删除: average...ean values of start ... [4]

.187
.188
.189
.190
.191
.192
.193
.194
.195
.196
.197

Table 3. The mean values of start time (units: LST), peak time (units: LST) and duration (units: hours) of heavy rainfall respectively on the conditions with more absorbing aerosols (AAI more than 75th percentile), more scattering aerosols (SAI more than 75th percentile), less or more BC (AOD of BC less than 25th or more than 75th percentile), less or more sulfate (AOD of sulfate less than 25th or more than 75th percentile), and their differences. Numbers in the brackets stand for the standard deviations on the means. All differences have passed the significant test of 95%.

Clean/Polluted	CF	CTP	COT		CWP		CER		
			liquid	ice	liquid	ice	liquid	ice	
AOD	Clean	62.8 (17.6)	442.3 (149.6)	6.9 (4.5)	6.7 (8.5)	62.8 (36.6)	123.1 (168.9)	16.7 (4.4)	32.0 (8.7)
	Polluted	89.3 (12.9)	487.3 (145.7)	10.0 (5.8)	12.9 (17.0)	96.4 (52.5)	211.3 (279.3)	17.5 (3.5)	29.2 (9.0)
CDNC	Clean	94.5 (6.1)	398.0 (131.7)	8.1 (6.0)	8.7 (10.6)	102.4 (104.3)	171.6 (204.3)	20.4 (2.8)	34.2 (6.0)
	Polluted	97.4 (4.2)	430.8 (135.2)	40.4 (21.5)	33.1 (22.7)	318.2 (213.2)	542.5 (447.8)	12.2 (1.9)	25.4 (8.7)

思媛周 19/7/21 12:02 AM

Clean/Polluted	CF
Clean (AOD)	62.8
Polluted (AOD)	89.3
Difference [P - C] Percentage [(P-C)/C]	26.5 42.2%
Clean (CDNC)	94.5
Polluted (CDNC)	97.4
Difference [P - C] Percentage [(P-C)/C]	2.9 3.1%

已删除:

思媛周 19/7/21 12:02 AM

已删除: average...ean values of CF ... [5]

.198
.199
.200
.201
.202
.203
.204
.205
.206

Table 4. The mean values of CF (units: %), CTP (units: hPa), COT (liquid and ice, units: none), CWP (liquid and ice, units: g/m²) and CER (liquid and ice, units: μm) on the clean condition (less than 25th percentile) and polluted condition (more than 75th percentile) using two indicators of AOD and CDNC. Numbers in the brackets stand for the standard deviations on the means. The differences between clean and polluted conditions have all passed the significant test of 95%.

.225

Group (case number)	CF	CTP	COT		CWP		CER	
			liquid	ice	liquid	ice	liquid	ice
1 Clean, dry (153)	93.8 (6.1)	393.3 (117.3)	7.2 (4.6)	7.6 (9.4)	88.7 (70.6)	149.0 (146.4)	20.4 (3.0)	36.7 (6.6)
2 Polluted, dry (128)	95.6 (5.1)	475.7 (142.8)	50.2 (24.4)	43.4 (19.3)	424.6 (275.5)	793.5 (404.7)	12.6 (2.4)	30.0 (7.0)
3 Clean, wet (155)	<i>92.7 (7.0)</i> <i>p_{1,3}>0.05</i>	457.4 (191.0)	8.6 (4.7)	10.6 (12.6)	101.9 (64.5)	207.7 (254.1)	<i>19.8 (2.5)</i> <i>p_{1,3}>0.05</i>	33.2 (4.4)
4 Polluted, wet (194)	97.8 (4.4)	<i>419.7 (141.0)</i> <i>p_{3,4}>0.05</i>	36.4 (20.6)	28.4 (21.1)	295.9 (208.7)	456.4 (412.1)	<i>12.5 (2.0)</i> <i>p_{2,4}>0.1</i>	24.4 (7.5)

.226

.227

.228

.229

.230

.231

.232

.233

.234

.235

.236

.237

.238

.239

.240

.241

.242

.243

.244

.245

.246

.247

.248

.249

.250

.251

.252

Table 5. The mean values of CF (units: %), CTP (units: hPa), COT (liquid and ice, units: none), CWP (liquid and ice, units: g/m²) and CER (liquid and ice, units: μm) in four groups. Numbers in the brackets stand for the standard deviations on the means. Italic numbers in grey represent that the differences are not significant, in which “P>0.05” stands for the difference has passed the significance test of 90% but did not pass the significance test of 95%, and “P>0.1” stands for the difference did not pass the significance test of 90%.

思媛 周 19/7/21 12:02 AM

Group (case number)	CF
1.Clean, dry (153)	93.8
2.Polluted, dry (128)	95.6
3.Clean, wet (155)	92.7 <small>0.05<p_{1,3}<0.1</small>
4.Polluted, wet (194)	97.8

已删除:

思媛 周 19/7/21 12:02 AM

已删除: average

思媛 周 19/7/21 12:02 AM

已删除: Grey

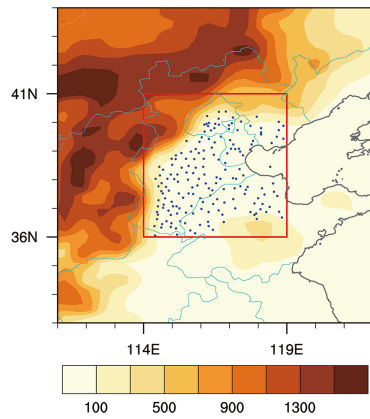
思媛 周 19/7/21 12:02 AM

已删除: <P<0.1

.257

.258 **Figures**

.259



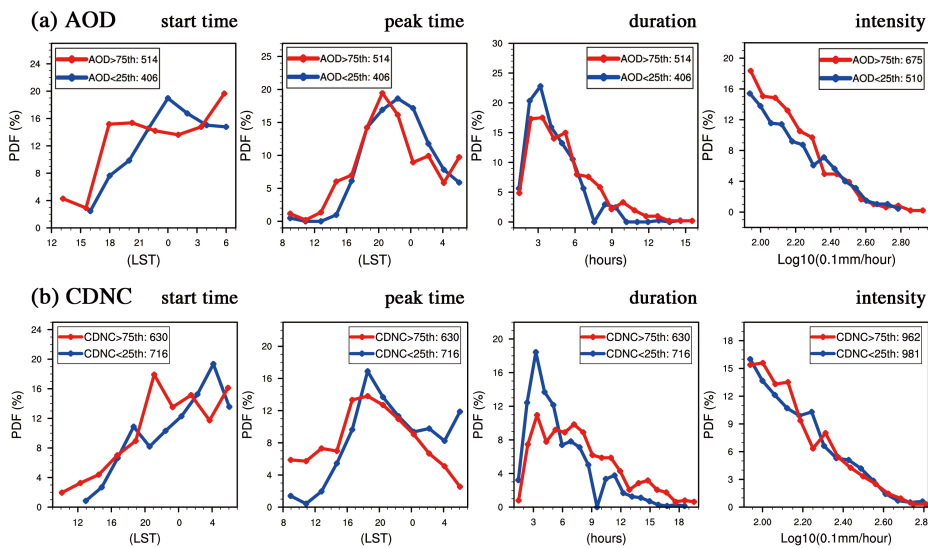
.260

.261 Figure 1. Altitudes (shading, units: m) and selected stations (dots) in the BTH region (red box, 36–41° N,

.262 114–119° E).

.263

.264



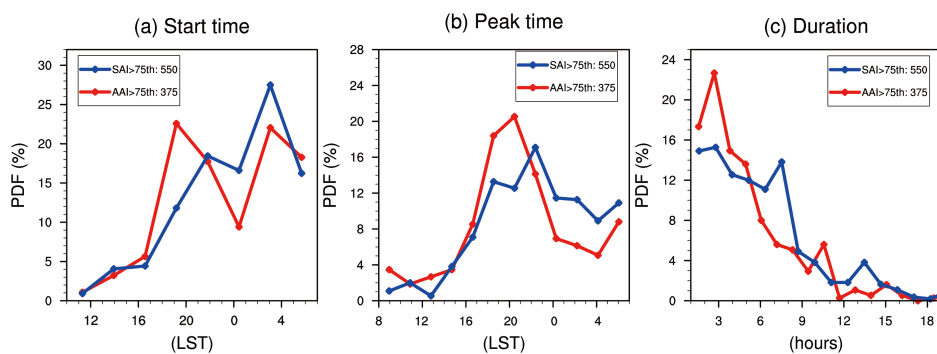
.265

.266 Figure 2. PDF of start time (units: LST), peak time (units: LST), duration (units: hours) and intensity (units:

.267 0.1mm/hour) of heavy rainfall on selected clean (blue lines) and polluted (red lines) conditions, respectively

.268 using indicator of (a) AOD and (b) CDNC (cm^{-3}), during early summers from 2002 to 2012.

.269



.270

.271 Figure 3. PDF of (a) start time (units: LST), (b) peak time (units: LST), and (c) duration (units: hours) of
.272 heavy rainfall on the days with SAI more than 75th percentile (blue lines) and days with AAI more than 75th
.273 percentile (red lines), during early summers from 2005 to 2012.

.274

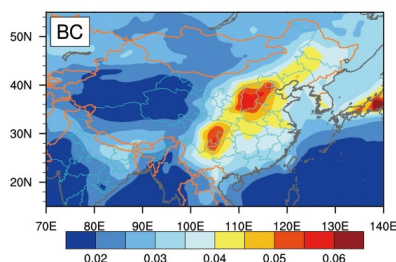
.275

.276

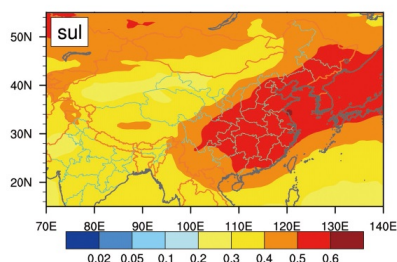
.277

- 思媛 周 19/7/21 12:02 AM
- 已删除: that
- 思媛 周 19/7/21 12:02 AM
- 已删除: tercile
- 思媛 周 19/7/21 12:02 AM
- 已删除: that
- 思媛 周 19/7/21 12:02 AM
- 已删除: tercile
- 思媛 周 19/7/21 12:02 AM
- 已删除: The differences between two groups have all passed the significant test of 95%.

(a) Percentage of BC AOD



(b) Percentage of sulfate AOD

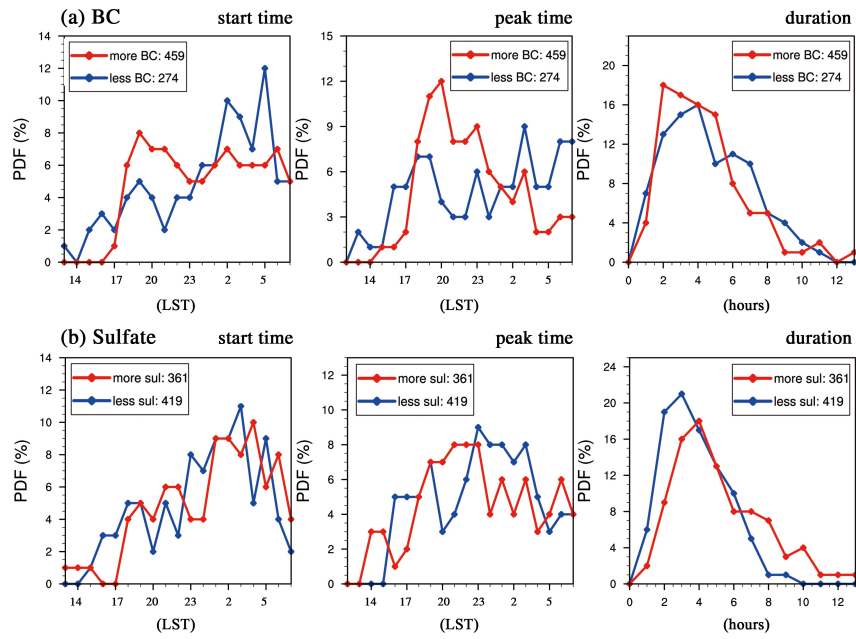


.278

.279 Figure 4. Percentages of AOD for (a) BC and (b) sulfate in JJA during 2002 to 2012.

.280

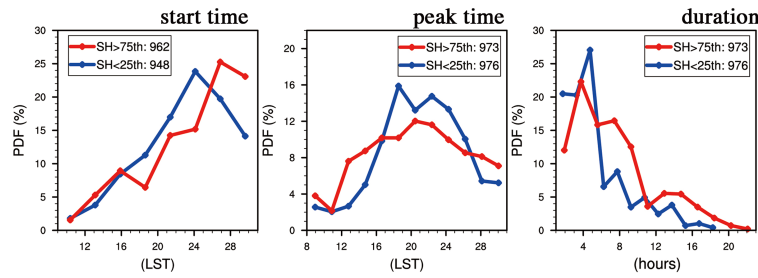
.281



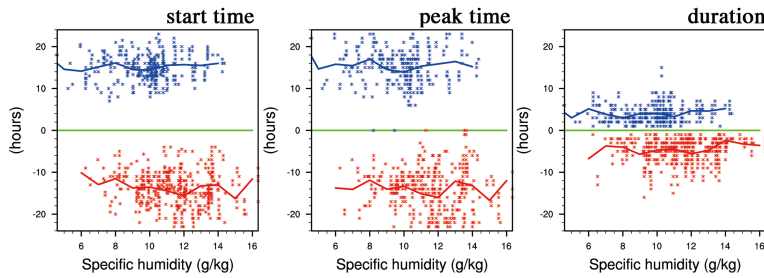
.288
.289 Figure 5. PDF of start time (units: LST), peak time (units: LST) and duration (units: hours) of heavy rainfall in
.290 different conditions of (a) BC and (b) sulfate. Blue/red lines stand for the condition of less/more BC or sulfate
.291 (AOD of BC or sulfate less than 25th/more than 75th percentile) during early summers from 2003 to 2012.

思媛 周 19/7/21 12:02 AM
已删除: The differences have passed the significant test of 95%.

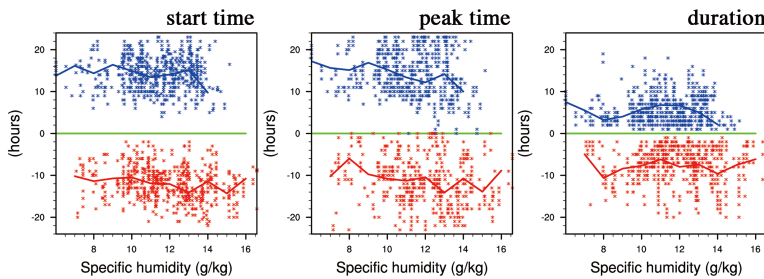
(a) PDF with more/less SH



(b) Scatter distribution using AOD



(c) Scatter distribution using CDNC



.299

.300

.301

.302

.303

.304

.305

.306

.307

.308

.309

Figure 6. (a) PDF of start time (units: LST), peak time (units: LST), and duration (units: hours) of heavy rainfall with less moisture (blue lines, SH at 850 hPa less than 25th percentile) and more moisture (red lines, SH at 850 hPa more than 75th percentile). (b) and (c) are scatter distributions of SH-start time/peak time/duration for clean cases (blue points) and polluted cases (red points) respectively using AOD and CDNC. Green lines stands for the start/peak time at 8:00 LST or duration is 0 hours. Positive (negative) values stand for the hours away from 8:00 LST or 0 hours in clean (polluted) cases. Blue (red) lines stand for the mean values of rainfall characteristics at each integer of SH in clean (polluted) cases.

思媛 周 19/7/21 12:02 AM
已删除: in different conditions of
思媛 周 19/7/21 12:02 AM
已删除: tercile
思媛 周 19/7/21 12:02 AM
已删除: tercile

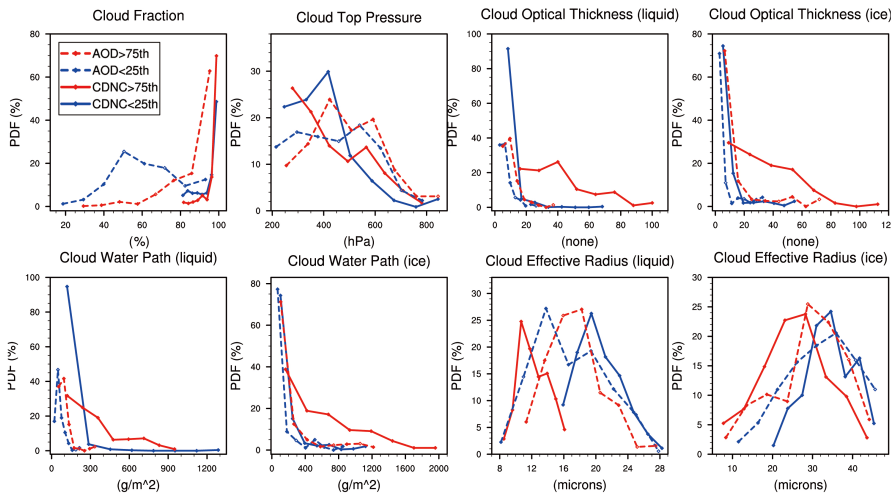


Figure 7. PDF of CF (units: %), CTP (units: hPa), COT (liquid and ice, units: none), CWP (liquid and ice, units: g/m^2) and CER (liquid and ice, units: μm) on selected clean (blue dash lines: AOD < 25th percentile; blue solid lines: CDNC < 25th percentile) and polluted (red dash lines: AOD > 75th percentile; red solid lines: CDNC > 75th percentile) heavy rainfall days.

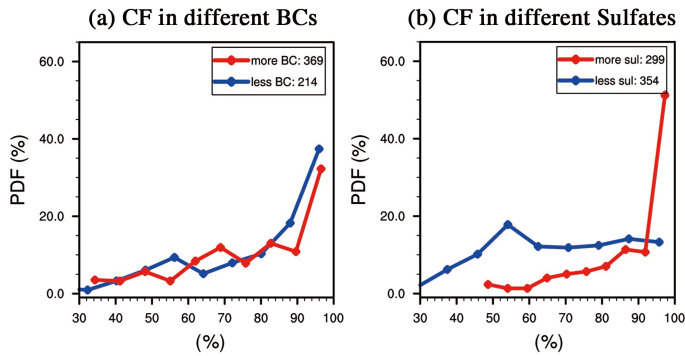
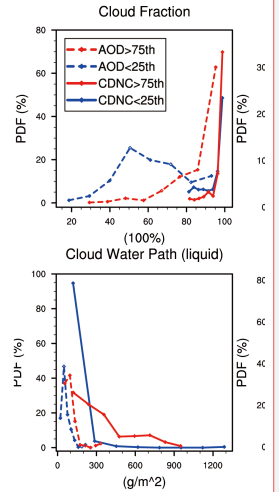


Figure 8. PDF of CF (units: %) respectively for the conditions of less BC/sulfate (blue lines, AOD of BC/sulfate less than 25th percentile) and more BC/sulfate (red lines, AOD of BC/sulfate more than 75th percentile) cases with heavy rainfall during 10 early summers (2003-2012).

思媛周 19/7/21 12:02 AM



已删除:

思媛周 19/7/21 12:02 AM

已删除: tercile

思媛周 19/7/21 12:02 AM

已删除: tercile

思媛周 19/7/21 12:02 AM

已删除: tercile

思媛周 19/7/21 12:02 AM

已删除: tercile

思媛周 19/7/21 12:02 AM

已删除: tercile

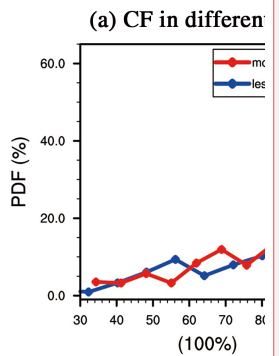
思媛周 19/7/21 12:02 AM

已删除: tercile

思媛周 19/7/21 12:02 AM

已删除: The differences between clean and polluted cases have all passed the significant test of 95%.

思媛周 19/7/21 12:02 AM



已删除:

思媛周 19/7/21 12:02 AM

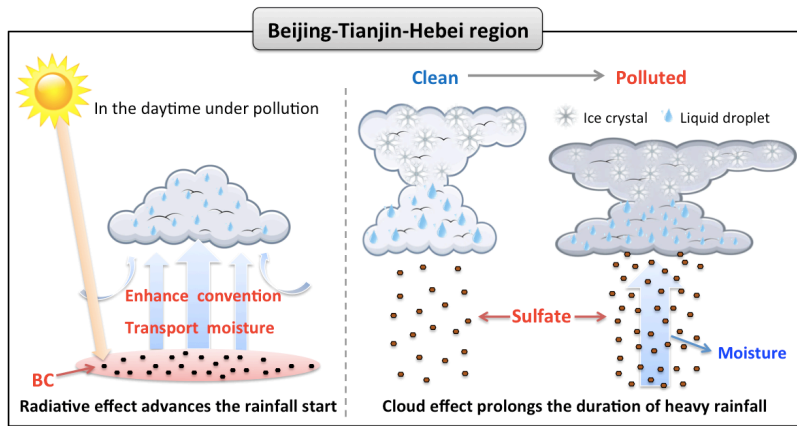
已删除: 100

思媛周 19/7/21 12:02 AM

已删除: selected

.338

.339



.340

.341 | Figure 9. A schematic diagram for aerosol impacts on heavy rainfall over Beijing-Tianjin-Hebei region.

.342

.343

.344

思媛 周 19/7/21 12:02 AM

已删除: aerosols impact